Carbohydrate Polymers 250 (2020) 116996

Contents lists available at ScienceDirect

Carbohydrate Polymers

journal homepage: www.elsevier.com/locate/carbpol

Exploring role of probiotics and *Ganoderma lucidum* extract powder as solid carriers to solidify liquid self-nanoemulsifying delivery systems loaded with curcumin

Rubiya Khursheed [a], Sachin Kumar Singh [a,*], Sheetu Wadhwa [a], Monica Gulati [a], Ankit Awasthi [a], Rajan Kumar [a], Arya Kadukkattil Ramanunny [a], Bhupinder Kapoor [a], Pushpendra Kumar [b], Leander Corrie [a]

[a] School of Pharmaceutical Sciences, Lovely Professional University, Phagwara, 144411, Punjab, India
[b] School of Chemical Engineering and Physical Sciences, Department of Chemistry, Lovely Professional University, Phagwara, 144411, Punjab, India

ARTICLE INFO

Keywords:
Curcumin
Ganoderma lucidum extract powder
Probiotics
Solid-SNEDDS
Spheroids

ABSTRACT

Solid self-nanoemulsifying drug delivery system (S-SENDDS) containing Curcumin (CRM) were prepared using combination of *Ganoderma lucidum* extract powder (GLEP) and probiotics (PB) as carriers. Liquid SNEDDS containing CRM were prepared by mixing Capmul MCM, Labrafil M1944CS, Tween 80 and Transcutol P. These were further spray dried and finally converted into spheroids. The droplet size of reconstituted S-SNEDDS powder and spheroids was found in the range of 35 to 37 nm, zeta potential in the range of - 21.48 to -23.22 mV and drug loading in the range of 95-96%. The release of drug from formulations was found to be more than 90%. Similarly, significant improvement ($p < 0.05$) in permeability of CRM was observed through SNEDDS using Caco2 cell lines. The non-significant difference ($p > 0.05$) in drug loading, droplet size, dissolution rate and angle of repose between L-SNEDDS and S-SNEDDS indicated the potential of GLEP-PB to produce stable SNEDDS.

1. Introduction

Development of an oral formulation containing lipophilic drugs has been a consistent challenge for formulation scientists because these drugs possess dissolution rate limited oral absorption and bioavailability (Brown et al., 2004; Gowthamarajan & Singh, 2010; Sachin Kumar Singh et al., 2011). The issue becomes even more cumbersome when the drug gets degraded in the gastrointestinal tract (GIT) (B. Kumar et al., 2018). A large number of formulation strategies have been explored to improve the dissolution rate and gastrointestinal (GI) stability of such drugs. These include formulation of nanosuspension (Mahesh, Singh, & Gulati, 2014), complexes (Danki & Thube, 2010; Singh, Pathak, & Bali, 2012; Singh, Srinivasan, Gowthamarajan et al., 2012; Singh, Srinivasan, Singare, Gowthamarajan, & Prakash, 2012; Zoeller, Dressman, & Klein, 2012), solid lipid nanoparticles (V. V. Kumar et al., 2007), solid dispersions (Kaur, Singh, Garg, Gulati, & Vaidya, 2015), liquisolid compacts (Jyoti et al., 2019; Singh, Srinivasan, Gowthamarajan et al., 2012), metastable polymorphs (Renuka, Kumar, Gulati, & Kaur, 2014), co-crystals (Pandey et al., 2017), metallic nanoparticles (Kumari et al., 2020) etc. However, these techniques have certain limitations such as toxicity and low stability etc. In recent years, liquid self-nanoemulsifying drug delivery systems (L-SNEDDS) have been reported as potential nanocarriers for delivering lipophilic and gastrointestinal labile drugs through oral route with improved bioavailability (Beg et al., 2016; Garg et al., 2017, 2019; Ghosh et al., 2020; Inugala et al., 2015; J. H. Kang, Oh, Oh, Yong, & Choi, 2012; Kazi et al., 2019; Khan, Kotta, Ansari, Sharma, & Ali, 2015; R. Kumar et al., 2019; Mohsin et al., 2016; Sharma et al., 2018). These L-SNEDDS, upon getting mixed with GI fluids get self-emulsified and form oil and water emulsion. The drug gets encapsulated in the emulsion droplets, gets solubilized at molecular level and gets absorbed through lymphatic route (Shakeel, Haq, Alanazi, & Alsarra, 2014). Thereby, it gets protected from GI fluids as well as hepatic first pass metabolism (Ghai & Sinha, 2012). Despite having such a great potential in overcoming poor aqueous solubility and oral bioavailability of drugs, L-SNEDDS suffer from some challenges such as difficulty in handling, transportation issues, palatability, dose variation as a unit dosage form as well as stability issues due to their liquid nature (Kamel & Mahmoud, 2013; J. H. Kang et al., 2012; Singh,

* Corresponding author.
E-mail address: sachin.16030@lpu.co.in (S.K. Singh).

https://doi.org/10.1016/j.carbpol.2020.116996
Received 29 April 2020; Received in revised form 22 August 2020; Accepted 23 August 2020
Available online 29 August 2020

Pathak et al., 2012; Sandeep Kumar Singh, Prasad Verma, & Razdan, 2010). Solid SNEDDS are easier to transport, more stable and amenable to compression to be formulated as tablets as compared to their liquid counter-parts. In order to overcome the challenges related to L-SNEDDS, various attempts have been made to solidify them. These include their adsorption on solid porous carriers using conventional adsorption technique, spray drying and pelletization technique (Beg et al., 2016; J. H. Kang et al., 2012; B. Kumar et al., 2018). For solidification, the most extensively used solid carrier is silicon dioxide (SiO_2) or its modified forms (Beg et al., 2016; B. Kumar et al., 2018; B. Singh, Bandopadhyay, Kapil, Singh, & Katare, 2009). The other carriers that have been used to solidify L-SNEDDS include lactose, Microcrystalline Cellulose (MCC PH102), magnesium stearate and talc. However, the amount of these carriers required to convert L-SNEDDS into free-flowing powder is generally quite high (i.e. minimum 2 g to 4 g/0.5 mL of L-SNEDDS) (Beg et al., 2016; Garg et al., 2017; B. K. Kang et al., 2004). Hence, the total weight of unit dosage form increases above 1 g. It becomes cumbersome for such quantities of powders to be compressed into tablets or, fill them into capsules as well as to administer them as unit dosage forms. SiO_2 and its modified forms have very large surface area as they are more porous in nature as compared to other hydrophilic or hydrophobic carriers (J. H. Kang et al., 2012; B. Kumar et al., 2018). Hence, they are able to solidify the L-SNEDDS in comparatively less amount as compared to that of any other hydrophilic or, hydrophobic carriers (Muthyala et al., 2016). However, SiO_2 poses some challenges such as non-biodegradability, potential clinical toxicity and poor compressibility (Lin, Huang, Zhou, & Ma, 2006; Malvindi et al., 2012). Moreover, usage of silica based nanoparticles, even at micron level has been reported to lead to autoimmune disorders such as lupus, silicosis, renal failure, lung cancer, rheumatoid arthritis and systemic sclerosis (Malvindi et al., 2012). Hence, the use of silica should be avoided in pharmaceutical formulations.

Since thousands of years, mushrooms are being used as edible material with medicinal value (Khanna, 2011; Khursheed, Singh, Wadhwa, Gulati, & Awasthi, 2020). The main polysaccharide present in mushrooms is reported to be beta-D-glucan which is well reported for its beneficial role in treating metabolic diseases such as obesity, diabetes, atherosclerosis, gut dysbiosis and cancer (Jeong et al., 2010; Khanna, 2011; Khursheed et al., 2019; Li, Zhang, & Ma, 2010). These are also reported to have antiviral, immunomodulatory, antibacterial and antifungal properties (Wasser, 2017). Probiotics (PB) are well known for managing gut dysbiosis and decreasing insulin resistance by decreasing secretion of lipopolysaccharides and thereby managing type 2 diabetes mellitus (Khursheed et al., 2019). Looking at the multiple health benefits of the polysaccharides obtained from *Ganoderma lucidum* extract (GLE) and PB, collectively forming a synbiotic, an attempt has been made to explore them as a biosorbent for conversion of L-SNEDDS to solid-SNEDDS (S-SNEDDS). It is pertinent to add here that synbiotics are combinations of probiotics and prebiotics with an inherent property to reverse dysbiosis, resulting in treatment of a number of intestinal and non-intestinal disorders. Furthermore, they are cost-effective, biodegradable, non-toxic and easily available worldwide. This is the first report of exploring any synbiotic combination for converting L-SNEDDS into S-SNEDDS.

Curcumin (CRM) has been used as model lipophilic and gastrointestinal labile drug to investigate the effect of developed formulation in enhacing its dissolution rate and permeability. CRM belongs to Biopharmaceutical Classification System (BCS) class IV, and has low aqueous solubility (3 mg/L in water) as well as membrane permeability (B. Kumar et al., 2018).

This study was undertaken based on the hypothesis that by solubilizing the lipophilic drug CRM, into the isotropic mixture of L-SNEDDS followed by its solidification into free flowing powder by spray drying on the mixture of GLE powder (GLEP) and PB, will increase its dissolution rate and permeability. Solidification of L-SNEDDS using GLEP-PB as solid porous carrier followed by their conversion into pellets would offer a novel, environment friendly, scalable and stable solid product. Based on the fact that mushroom polysaccharides act as prebiotics (Khan et al., 2018), their combination with PBs is anticipated to restore the gut microbiota, eventually leading to a beneficial effect on metabolic diseases (Hur & Lee, 2015).

2. Materials and methods

2.1. Materials

CRM was purchased from Molychem, Mumbai, India. Propylene glycol (PG), Tween (T) 20 and 80, Polyethylene glycol (PEG) 200, 400, and 600, Span 80, aerosil 200 (A-200), microcrystalline cellulose PH102 (MCC PH102), magnesium stearate (MS), sucrose, glucose, sodium chloride, hydrochloric acid and lactose were purchased from Central Drug House, New Delhi, India. Sesame oil, soyabean oil, groundnut oil, cotton seed oil, almond oil, eucalyptus oil, mustard oil, olive oil, castor oil were purchased from Global Merchants, Navi Mumbai, India. Labrafac PG (LPG), Labrafil M1944CS (LMCS), Lauroglycol FCC (LFCC), Labrasol (LS), and Transcutol P (TP) were gifted by Gattefosse, Mumbai, India. Capmul MCM (CMCM) was gifted by Abitec Corp., Mumbai, India. Acetonitrile (ACN, HPLC grade) was purchased from Rankem, Mumbai, India. Glacial acetic acid (GAA) was purchased from Loba Chemie, Mumbai, India. GLEP was gifted by Ayush Herbal and Healthcare, Sirmour, India. As per the certificate of analysis the GLEP contained 60% β-D-glucan, having molecular weight of 22014 Da. The structure of beta-D-glucan present in GLEP is shown in supplementary file **Fig. S1**. PB (More Biotic) having composition *Bacillus mesentericus (15 million cells), Clostridium butyricum (15 million cells), Lactobacillus acidophilus (15 million cells), Streptococcus thermophilus (15 million cells) and Fructooligosaccharides (100 mg),* was purchased from Dr Morepen Laboratories Ltd. Delhi, India. Casein-peptone Soymeal-peptone (CASO) and MRS-Clindamycin-Ciprofloxacin (MRS-CC) media and Folin-Ciocalteu's phenol reagent (FCR) were purchased from Merck, Darmstadt, Germany. Meat extract, peptone, iron sulfate, biotin, cysteine hydrochloride, glucose, agar, trimethoprim, cycloserine, and polymyxin B sulfate were purchased from HiMedia, New Delhi, India. The phenolic standards kaempferol, naringenin, quercetin, rutin, chlorogenic acid, syringic acid, *trans*-cinnamic acid, resveratrol, vanillic acid, *p*-hydroxybenzoic acid, caffeic acid, benzoic acid, gallic acid and *p*-coumaric acid were purchased from Sigma Aldrich, Steinheim, Germany. Catechin and hesperetin were purchased from Merck, Darmstadt, Germany. All the reference standards used were of 99% purity. Triple distilled water was used throughout the study. Spray dryer from SprayMate, Jay Instruments and systems, Navi Mumbai, India was used in the study. Extrusion spheronizer (UICE-LAB) and mini fluidized bed dryer (FBD) were purchased from Umang Pharmatech, Palghar, India. High-Performance Liquid Chromatography (HPLC) system (LC-20 AD; Shimadzu, Japan), fitted with photodiode array detector (SPDM20A; Shimadzu, Japan) was used for quantitative analysis of the drug. Magnetic Stirrer, MS500, REMI, New Delhi, India was used for mixing of solutions. UV-visible double beam spectrophotometer, UV-1800, Shimadzu, Japan was used for recording absorbance of samples. Dissolution apparatus DS8000, Lab India, Mumbai, India was used to carry out release studies. Vortex mixer, CM 101 CYCLO MIXER, REMI, New Delhi, India was used for solubility studies and preparation of isotropic mixtures. Shaking water bath, LABFIT, India was used for solubility studies. Centrifuge, REMI CM-12 PLUS, New Delhi, India was used for centrifugation of samples. Tap density apparatus, USP type, Electro lab Pvt. Ltd., Mumbai, India was used. Zeta sizer Nano ZS90 (Malvern Instruments Ltd., UK) was used for droplet size and zeta potential analysis. Differential Scanning Calorimeter, DSC Q200 TA, Universal instrument, Bangalore, India was used to record thermograms. X-ray diffractometer, Bruker axs, D8 Advance was used for determination of X-ray diffractograms of powder samples. Transmission electron microscope (TEM; H-7500, Hitachi, Japan) was used to determine surface morphology of SNEDDS droplets.

Scanning electron microscope, JSM6100, JEOL India Pvt. Ltd, New Delhi, India was used for microscopic structural determination of powders.

2.2. Characterization of GLEP

2.2.1. Determination of total phenolic contents

The total phenolic content (TPC) present in GLEP was determined by the Folin-Ciocalteu's method described by Singleton and Rossi (Singleton & Rossi, 1965). In brief, 1 g of GLEP, 60 mL of distilled water and 5 mL FCR were taken in 100-mL volumetric flask and mixed well. After 1 min and before 8 min, 20% w/v sodium carbonate solution (15 mL) were added and the volume of solution was adjusted to 100 mL using distilled water. The solution was kept aside for 2 h at about 23 ℃. Similarly, a blank solution was also prepared in similar way without addition of GLEP. At the end of 2 h, the absorbance of solution was recorded at 760 nm using UV-visible double beam spectrophotometer against blank. Determination of phenolic compounds was done by the HPLC method using HPLC. Chromatographic separation was carried out on C-18 column (Nucleodur C18, 250 mm × 4.6 mm i.d.,5μ). The solvent system had a constant flow rate of 1.0 mL/min. The mobile phase was distilled water with 0.1% v/v GAA as solvent A and ACN with 0.1 % v/v GAA as solvent B. The elution was carried out in gradient mode for 30 min as: 0 to 3.25 min, 8 to 10 % B; 3.25 to 8 min, 10 to 12% B; 8 to 15, 12 to 25 % B; 15 to 15.8 min, 25 to 30% B; 15.8 to 25 min, 30 to 90% B; 25 to 25.4 min, 90 to 100% B; 25.4 to 30 min, 100 % B. Injection volume was 20 μL and temperature was kept constant at 25℃. The wavelengths of detection were chosen according to absorption maximum of analyzed phenolic compounds. It was chosen 225 nm for vanillic acid as well as benzoic acid, 280 nm for gallic acid, catechin, *p*-hydroxybenzoic acid, syringic acid, trans-cinnamic acid, hesperetin, naringenin, 305 nm for coumaric acid as well as resveratrol, 330 nm for caffeic acid as well as chlorogenic acid and 360 nm for rutin, quercetin as well as kaempferol. External standard method was used to quantify compounds (Veljović et al., 2017). Quantification was performed by external standard method. The standard stock solutions were prepared in the range of 1, 2.5, 5, 10, 15, 25 μg/mL. The dilutions were prepared with dimethyl sulfoxide (DMSO). All standard calibration curves were found linear with coefficient of determination (r^2) as 0.999. Samples were filtered through 0.45 μm filter and injected to HPLC.

2.2.2. Measurement of glucan content

Mushroom and Yeast β-glucan assay procedure (Mega zyme Int.) was used to determine the contents of total and α-glucans present in the GLEP. The method described by Kozarski, Klaus, and Nikšić (2012)) was followed for estimation of glucans. The β-glucan content was calculated by subtracting the α-glucan from the total glucan content. All values of glucan contents were expressed as g/100 g of a dry weight (DW) of the Megazym program Mega-CalcTM (Kozarski et al., 2012).

2.3. HPLC analytical method

The reverse phase HPLC method was developed using ACN and GAA as mobile phase with gradient method of elution at a flow rate of 1.0 mL/min. C-18 column (Nucleodur C18, 250 mm × 4.6 mm i.d.,5μ) was used as stationary phase. The detection wavelength was 420 nm. The run time for elution was kept as 15 min. A gradient method having ratio of GAA: ACN 60:40 v/v for first five min followed by 40:60 v/v between 5-8 min and 20:80 v/v between 8-15 min was used. Samples (20 μL) were injected into the system and development of chromatogram was monitored through LC solution software. Calibration curve was developed in the range of 2-10 μg/mL. Retention time for CRM was found to be at 12.1 min. The resulting standard curve was found to be linear with coefficient of determination (r^2) as 0.999. Specificity study was carried out to check any possible interaction of excipients with CRM. Specificity was evaluated by analysing the chromatograms of placebo solutions of all the solubilizers and excipients used for formulating SNEDDS, as well as SNEDDS placebo at concentration of 10 μg/mL. The placebo solution was prepared with the same composition as the SNEDDS formulation without the addition of CRM and treated in the same manner as the sample solution and the reference solution.

2.4. Solubility studies

Solubility study was carried out for selection of solubilizers in which drug should have maximum solubility for preparation of isotropic mixture of SNEDDS. A known excess of CRM (50 mg) was added to glass vials of 5 mL capacity containing 1 mL of individual oils (castor oil, sesame oil, groundnut oil, LFCC, eucalyptus oil, cotton seed oil, PG, olive oil, soyabean oil, LMCS, LPG, almond oil, CMCM, and mustard oil) and surfactants (LS, PEG 200, PEG 400, PEG 600, PG, T20 and 80, span 80, TP) respectively. To a mixture of 1 mL each of oil, surfactant and co-surfactant, a known excess amount of drug was added and vortexed for 5 min. Then these vials were stoppered and agitated for 48 h at 37 ± 0.2 ℃ in a shaking water bath. Upon equilibration, all the samples were centrifuged at 9626 *g* for 20 min for removal of any undissolved drug from the saturated solutions. The supernatants were taken and appropriately diluted with ethanol or hexane (depending upon the miscibility of solubilizer) and drug concentration was measured by HPLC (R. Kumar et al., 2019).

2.5. Formulation of L-SNEDDS

It is pertinent to add here that initially only LMCS was used as oil as CRM exhibited highest solubility in it. T80 was used as surfactant and TP as co-surfactant. Total 27 SNEDDS formulations were prepared by varying oil and surfactant-cosurfactant mixture (Smix) in the ratio of 1:9, whereas, the internal composition of Smix was varied in the ratio of 1:1, 1:2 and 2:1. The results are shown in supplementary data as **Table S1** and **Fig. S2**. Out of 27 formulations, only 2 formulations, SF1 and SF10 showed clear transparent emulsion. Hence, we can say that a poor nanoemulsion zone was obtained. The mean droplet size, polydispersity index (PDI) and zeta potential for SF1 and SF10, were found to exhibit size above 130 nm (138.41 ± 3.42 nm for SF1 and 154.32 ± 5.67 nm for SF10), PDI above 0.3 (0.36 ± 0.09 for SF1 and 0.42 ± 0.05 for SF10) and zeta potential below – 15 mV (- 9.16 ± 1.16 mV for SF1 and - 11.22 ± 2.17 mV for SF10). The objective of present study was to control mean droplet size below 50 nm for better permeation of CRM through GIT and zeta potential above - 15 mV in order to keep the nanoemulsion stable. Apparently, this could not be met using LMCS. Hence, another oil, CMCM was also incorporated in the study. The solubility of CRM in CMCM was almost 54 ± 2.22 % times as that of LMCS, hence, formulation of SNEDDS using CMCM as oil alone was not tried.

The L-SNEDDS were prepared using varying ratios of CMCM, LMCS, T80 and TP. CMCM and LMCS were used as Omix and their ratio was varied in the range of 1:1, 1:2 and 2:1. Similarly, T80 and TP were used as Smix and also varied in the ratio of 1:1, 1:2 and 2:1. The Omix and Smix were varied in the ratio of 1:9 to 9:1. Using these ratios, a total of eighty one SNEDDS prototypes were prepared. The study was designed using ternary phase diagram and the region indicating the formation of clear and transparent emulsion without any phase separation or, precipitation was marked as SNEDDS and the emulsions appearing translucent were marked as SMEDDS. Emulsions showing creaming, cracking or, drug precipitation were marked as those exhibiting phase separation. Triplot software version 4.1.2. (Todd Thompson Software) was used to design the ternary phase diagram. The formula composition of SNEDDS prototype is shown in supplementary data as **Table S2**. Initially, the SNEDDS pre-concentrate (1 mL) was prepared for all batches by mixing the oil, surfactants and co-surfactants in the specified ratio, using vortex mixer for 15 min. This was followed by addition of CRM (25 mg) to each of the prepared pre-concentrate. Afterwards, the mixture was again vortexed for 15 min using vortex mixer. The prepared prototypes were

diluted using 500 mL distilled water. The mixture was stirred at 500 rpm at 37 ± 0.2 ℃ for 5 min.

2.6. Stability evaluation of L-SNEDDS prototypes

The L-SNEDDS should be thermodynamically and kinetically stable. The thermodynamic stability of formulations was evaluated by subjecting to cooling-heating cycles (4 ℃ and 40 ℃) and freeze and thaw cycles (-21 ℃ and +25 ℃) with storage for 48 h and cloud point determination. Kinetic stability of formulations was determined by centrifuging the diluted SNEDDS formulations at 10000 *g* for 15 min and observing creaming, cracking and drug precipitation (Inugala et al., 2015; Kallakunta, Bandari, Jukanti, & Veerareddy, 2012). In order to determine cloud point temperature, prepared formulations (1 mL) were diluted in 500 mL water and gradually heated on a temperature regulated digital water bath. The temperature of water was increased at a rate of 5 ℃/min from 25 ℃ to a temperature at which cloudiness appeared. The appearance of cloudiness was observed visually as the temperature at which the transparent emulsion started showing milky opalescence (B. Kumar et al., 2018; Zhang, Liu, Feng, & Xu, 2008).

2.7. Formulation of S-SNEDDS

2.7.1. Determination of loading factor (L_f)

The L_f helps in understanding the liquid absorption capacity of the solid carriers. The higher value of L_f signifies less requirement of carrier to provide free-flowing powder (Jyoti et al., 2019; Singh, Srinivasan, Gowthamarajan et al., 2012). This is calculated by dividing weight of liquid (W) by weight of carrier (Q) required to solidify them. The L_f of GLEP, PB and GLEP-PB in the ratio of 1:1 was calculated for solidifying L-SNEDDS pre-concentrates. In addition to that, the L_f value of some of the other widely used carriers such as lactose, A-200, MCC PH102 and MS for solidifying S-SNEDDS was also calculated. To calculate L_f, L-SNEDDS (0.5 g) were taken in a mortar and weighed amounts of solid carriers were added and blended gently by pestle. Addition of solid carriers was continued till free-flowing powder was achieved.

2.7.2. Angle of repose

The flow properties were determined by calculating angle of repose (AOR) according to the procedure mentioned by Kaur et al., 2015 (Kaur et al., 2015) by standard funnel method. In brief, the funnel was fixed 4 cm above the bench surface. The prepared S-SNEDDS powder blends were poured individually through this funnel. The height (h) and radius (r) of the pile from the base were measured. The formula to calculate AOR (θ) is given in Eq. (1) (Kaur et al., 2015).

$$AOR\ (\theta) = \frac{tan - 1h}{r} \quad (1)$$

2.7.3. Spray drying of S-SNEDDS

The prepared S-SNEDDS powder blend was solidified further through spray drying. The S-SNEDDS powder blends (1 g) with various carriers, were mixed with suitable solvents and spray dried. Water (100 mL) was used as solvent to disperse GLEP, PB, GLEP-PB (1:1) and lactose, whereas, ethanol (100 mL) was used as solvent to disperse MCC PH102, A-200 and MS. Spray dryer was used to formulate spray dried S-SNEDDS. It is important to note that to ensure complete free flow, A-200 (0.2 g) was added as coating material to all the prepared dispersions prior to their spray drying. The dispersions were sprayed at an air pressure of 4 Kg/cm^2 through spray nozzle having 0.7 mm diameter at a flow rate of 20 mL/min using a peristaltic pump. The inlet air temperatures were kept at 70 ℃ and 100 ℃ and recorded outlet air temperatures were 35 and 50 ℃, for ethanol and water respectively.

2.7.4. Evaluation of survival rate of bacteriae present in probiotics

The probiotics blend was containing four different bacteriae viz. *Bacillus mesentericus, Clostridium butyricum, Lactobacillus acidophilus, Streptococcus thermophilus*. In order to check their survival rate, their total viable count pre and post spray drying was tested. For *Bacillus mesentericus,* the broth consisting of 10 mg/mL meat extract, 10 mg/mL peptone, 10 mg/mL sucrose and 15 mg/mL sodium chloride was used. The pH of the medium was adjusted to 7.0 (Ozone et al., 2002). For *Clostridium butyricum* the composition of medium includes concentrated mineral salts solution (100 mL), phosphate solution (100 mL), 0.1 % aqueous solution of iron sulfate (10 mL), 0.002% aqueous solution biotin (0.25 mL), cysteine hydrochloride (0.5 g), glucose (10 g), agar (15 g), trimethoprim (16 mg), cycloserine (10 mg), polymyxin B sulfate (20 mg), distilled water, 790 mL. The pH was adjusted to pH 7.7 (Popoff, 1984). For *Lactobacillus acidophilus,* MRS-CC agar media was used by rehydrating it in distilled water according to manufacturer's instructions, and adjusting its pH to 6.2 using hydrochloric acid (1 M HCl) at 25 °C (Süle, Kőrösi, Hucker, & Varga, 2014). Anaerobic conditions were generated using anaerobic culture jars (2.5 L) and AnaeroGen AN 25 sachets (Oxoid, Basingstoke, United Kingdom). For *Streptococcus thermophilus,* CASO broth was used. It included 17.0 g of pancreatic digest of casein, 3.0 g of papaic digest of soybean meal, 5.0 g of sodium chloride, 2.5 g of dipotassium hydrogen phosphate, 2.5 g of glucose, 1.0 g of skimmed milk powder, and 1000 mL of distilled water. The final pH of CASO broth was 7.3 at 25 °C. *Streptococcus thermophilus* was grown under aerobic condition at 37 °C for 48 h (Süle et al., 2014). All the media were autoclaved at 110 °C for 20 min.

In order to calculate the viable cell count, 1 g of the pre and post dried S-SNEDDS powder containing PB were taken in previously sterilized and warmed phosphate buffer saline (PBS) at 37 °C and the total volume was made 50 mL. This was diluted with PBS by a 10-fold dilution method so as to make the viable cell count 20-200 in 1 mL. This liquid (1 mL) was placed on four different petri dishes. To this, 20 mL of above prepared media (specific to the microorganism), SNEDDS powder (1 g) kept at 50 °C were separately added to each of the plates and mixed quickly and left undisturbed to solidify. This was subjected to incubation at 37 °C for 60 hours and viable cell count was determined from the appeared colony numbers and the diluting ratio. Survival rate was calculated using formula given in equation (2).

Survival rate (%) = {((viable cell count per gram of spray dried S-SNEDDS powder) × (solid content of the powder suspension)/ (viable cell count per gram of S-SNEDDS powder prior to drying)} × 100 Eq. (2)

2.8. Characterization of SNEDDS

2.8.1. Micromeritic evaluation of spray dried S-SNEDDS powders

The micromeritic parameters such as true density (TD), bulk density (BD), tapped density (TPD), flow rate, AOR and Carr's compressibility index (CCI) were measured. All the studies were carried out as reported by Kumar et al., 2018 (B. Kumar et al., 2018). Liquid displacement method using ethanol (as immiscible liquid) was used to calculate TD of powders. The TD (ρ_T) was calculated (n = 3) according formula given in Eq. (3).

$\rho T = \frac{W1}{W2+W1} - W3 \times sg$ Eq. (3)Here, W_1- powder' weight; sg – solvent's specific gravity; W_2 – bottle with solvent' weight; W_3 - bottle with solvent and powder's weight.

The powders were filled in the measuring cylinder attached with digital tap density apparatus. The volume of untapped powder was noted. Afterwards, the cylinder was tapped 100 times and volume of tapped powder was noted. Each study was carried out in triplicate. BD (ρb) and TPD (ρt) were calculated using the Eq. (4) and (5). CCI was calculated using formula given in Eq. (6). Determination of flow rate was done by calculating the ratio of mass (g) to time (s) by passing the powder through the glass funnel having an orifice of 10 mm diameter. AOR was determined as per the procedure described in section 2.6.2. All experiments were carried out in triplicate.

$$\text{BD } (\rho b) = \frac{Ms}{Vb} \quad (4)$$

$$\text{TPD } (\rho t) = \frac{Ms}{Vt} \quad (5)$$

$$CCI = \frac{\rho t - \rho b}{\rho t} \times 100 \quad (6)$$

2.8.2. Drug loading

The prepared L-SNEDDS (Optimized batch) and S-SNEDDS that were prepared using GLEP: PB (1:1) as solid carrier (GLEP-PB-S-SNEDDS) were subjected for percentage drug loading. The SNEDDS containing CRM (25 mg) were diluted with 500 mL of distilled water that was stirred at 500 rpm. From this dilution, 5 mL aliquots were taken and centrifuged at 10000 *g* for 15 min. The clear supernatant was taken and passed through 0.2 μm syringe filter and 20 μL sample was injected to HPLC. Percentage drug loading was calculated using formula given in Eq. (6).

$$\text{Drug Loading } (\%) = \frac{Sample\ area}{Standard\ area} \times 100 \quad (6)$$

2.8.3. Droplet size and zeta potential analysis

Droplet size and zeta potential of L-SNEDDS (Optimized batch) and GLEP-PB-S-SNEDDS were determined using zeta sizer by passing the laser light of 50 mV potential through the samples kept in polystyrene cuvettes at an angle of 90 degrees. The SNEDDS sample (0.1 mL) were diluted to 100 mL using distilled water and filtered using 0.2 μm syringe filter. The dilution (1 mL) was taken in the sample cell and analyzed. The operation was carried out at 25 ℃ (Ghosh et al., 2020).

2.8.4. Robustness to dilution and pH change

It is important that upon entering into the GIT, the SNEDDS should retain their size with varying pH and volume of the GI fluids from stomach to colon. In order to evaluate this, the prepared S-SNEDDS were diluted in four different media viz. water, 0.1 N HCl (pH 1.2), 0.1 M acetate buffer (pH 4.5) and phosphate buffer (0.2 M, pH 6.8). GLEP-PB-S-SNEDDS (1 mL) were diluted to 10, 100, 500 and 900 times in all the four media. The mean droplet size and phase separation was observed for all the diluted samples. Each study was carried out in triplicate and mean data was recorded.

2.9. Preparation of spheroids

In order to increase the physicomechanical stability and ease of handling, the GLEP-PB-S-SNEDDS powder were converted to spheroids using extrusion-spheronization technique. The advantages of converting powders into spheroids through extrusion-spheronization technique offers more convenience and uniformity while administration of the drug. Spheroids also are also known to possess excellent flow properties which would be useful during scale-up for automated processes or, in processes where exact dosing is required e.g. capsule filling and packaging. Moreover, the stability during storage and transport is reported to be more for spheroids as compared to that of powders (Ahir, Mali, Hajare, Bhagwat, & Patrekar, 2015; Deb & Ahmed, 2013). The powder (1.2 g) was blended with 0.5 g of MCC PH 101 and 0.5 g of lactose. The resulting blend was mixed with 2 % w/v starch solution (q.s.) in order to get wet cohesive mass. Afterwards 1% w/w talc was added. The extruder was set at speed between 20 to 98 rpm under controlled conditions. The prepared blend was transferred to the extruder via feeder hopper. The arm of extruder was rotated and the blend was passed through the perforated screen in order to get long extrudates. These extrudates were transferred to the spheronizer that was rotated at a speed of 200 rpm and a pressure of 1 bar. The speed of spheronizer was increased slowly from 200 rpm till 900 rpm in order to achieve spherical spheroids. The process was carried out for 15 min and water was sprinkled during the rotation in order to avoid agglomeration of prepared spheroids. Upon complete spheronization, the speed of spheronizer was brought down to 200 rpm and the process was stopped. The spheroids were taken out and dried using a fluidized bed drier at a temperature of 50 ℃. The speed of blower was kept at 2000 rpm and inlet temperature was kept at 70 ℃. The drying process was continued for 20 min and spheroids were taken out upon cooling of the drier. The scheme for formulating S-SNEDDS spheroids (MP-GLEP-S-SNEDDS) is shown in supplementary **Fig.S3**. The obtained spheroids were found to be spherical in shape with diameter less than 0.5 mm. The prepared GLEP-PB-S-SNEDDS spheroids were subjected to measurement of drug loading (%), droplet size and zeta potential as well as micromeritic evaluation as per the procedures mentioned in sections 2.7.1 to 2.7.3.

It is important to note that the entire process was operated in a sterile lab equipped with HVAC system and laminar air flow. Moreover, proper fumigation of lab was carried out prior to start of operation using suitable disinfectant.

2.10. Differential Scanning Calorimetry (DSC)

Raw CRM, GLEP, PB, A-200, CMCM, LMCS, T80, TP, GLEP-PB-S-SNEDDS powder (spray and non-spray dried) and GLEP-PB-S-SNEDDS spheroids were subjected to DSC analysis. Samples (2 mg) were weighed and crimped individually in aluminium pans. The thermograms of samples were recorded in the range of 0 to 300 ℃ at a heating rate of 10 ℃/min against an empty aluminium pan that was taken as reference standard. Nitrogen gas was continuously supplied at a flow rate of 50 mL/min during the analysis. The melting points (Tm) were determined using TA-Universal Analysis 2000 software (version 4.7A) (Kaur et al., 2015).

2.11. Powder X-ray Diffraction (PXRD) studies

The PXRD patterns of raw CRM, PB, GLEP, A-200, and GLEP-PB-S-SNEDDS powder (spray and non-spray dried) were recorded using an X-ray diffractometer. Copper line was used as source of radiation. The X-ray beams were incident on the sample at a voltage of 40-kV and current of 40-mA. The scanning rate of samples was maintained at $0.010^{\circ}min^{-1}$ over a 2θ range of 345 degrees (Kaur et al., 2015).

2.12. Microscopic analysis

The morphology of optimized L-SNEDDS and reconstituted GLEP-PB-S-SNEDDS (spray dried) droplets was observed using transmission electron microscopy. The samples (100 μL) were diluted to 10 mL using double distilled water. One drop of emulsion was taken and spread over carbon-coated copper grid for formation of film and kept for drying. Afterwards it was negatively stained using one drop of 2 % (w/v) phosphotungstic acid solution and air dried. Afterwards, they were subjected to TEM (Garg et al., 2017).

Scanning electron microscopy (SEM) was carried out to understand the surface morphology of raw CRM and surface transformation that occurred after its conversion into S-SNEDDS. SEM was carried out for raw CRM, PB, GLEP, A-200, and GLEP-PB-S-SNEDDS powder (spray and non-spray dried). Prior to analysis, the samples were fixed on a metallic stub using a conductive tape (12 mm diameter). The data station used was Supra 35 V P (Oberkochen, Zeiss, Germany). The voltage used to accelerate electrons was adjusted between 5-25 kV (Renuka, Kumar, Gulati, & Kaur, 2014).

2.13. Permeability studies

Permeability studies were carried out using Caco2 cell monolayer. Twenty-one days before conducting the study, these cells were cultured on Trans well polycarbonate membrane (12 mm length and 0.4 mm pore size) by supplying them transepithelial electrical resistance of 300

Ω/cm^2. Prior to the transcellular transport study, the cultured cells were washed thrice using Hank's balanced salt solution having pH 6.5. In the apical side (A) of cells, 0.5 mL of transport buffer was added. In the basolateral side (B), 1.5 mL of transport buffer was added. To carry out permeability study, raw CRM (25 mg) was suspended in a 0.2 % w/v solution of carboxy methyl cellulose. CRM loaded L-SNEDDS, CRM loaded GLEP-PB-S-SNEDDS spray dried powder and CRM loaded GLEP-PB-S-SNEDDS spheroids each containing CRM equivalent to 25 mg were diluted to 500 mL water. All of the above solutions (20 μM) were added into the "A" and "B" sides of cell. The study was carried out for five hours. At the end of every one hour, 0.1 mL sample was withdrawn from both the sides of cell and the withdrawn volume was replaced with equal volume of fresh transport buffer. These withdrawn samples were centrifuged at 10000 *g* for 10 min and filtered through 0.2 μm syringe filter and analyzed using HPLC at 420 nm. The amount of drug permeated with respect to time was noted (R. Kumar et al., 2019).

2.14. Dissolution studies

The raw CRM (25 mg), CRM loaded L-SNEDDS, CRM loaded GLEP-PB-S-SNEDDS powder and CRM loaded GLEP-PB-S-SNEDDS spheroids were subjected to dissolution studies in 900 mL of SGF (pH 1.2) maintained at 37 ± 0.2 ℃ for 60 min using USP type I basket apparatus. The baskets were rotated at 100 ± 4 rpm. All the SNEDDS formulations subjected to dissolution studies contained CRM equivalent to 25 mg. These SNEDDS were filled in size "000" capsule shells having 26.14 mm length and 9.91 mm external diameter. The samples were withdrawn at pre-determined time intervals of 5, 10, 15, 30, 45 and 60 min and the withdrawn medium was replaced by fresh medium for maintaining sink condition. The withdrawn samples were centrifuged at 10000 *g* for 10 min and clear supernatant was filtered through 0.2 μm syringe filters. The filtered samples were injected to HPLC and analyzed at 420 nm.

2.15. Stability studies

The GLEP-PB-S-SNEDDS powder and its spheroids were kept at 40 ℃ ± 2 ℃/ 75 % R.H. ± 5% R.H., in a stability chamber for six months. The parameters used to compare the performance of aged and fresh samples include droplet size (after diluting the sample using 500 mL of 0.1 N HCl, pH 1.2), drug loading (%), drug precipitation, AOR and drug dissolution. At the end of six months, all the mentioned parameters were compared between freshly prepared SNEDDS samples and aged one. The dissolution study was carried out as per the procedure mentioned in section 2.13. Each study was carried out six times and mean data (± s.d.) was recorded. The dissolution profiles were compared to find out possible changes in the formulation using similarity factor (f2) by model independent analysis. For two profiles to be considered statistically similar, the value of f2 should be above 50 (Shah, Tsong, Sathe, & Liu, 1998).

2.16. Statistical analysis

All the experimental results were expressed as mean ± standard deviation (SD). The comparison between results was done either by using one-way ANOVA or Tukey's multiple comparison test using GraphPad Prism version 7.0 (GraphPad Software Inc., CA, USA). A value of $P < 0.05$ indicated significant difference in the obtained results.

3. Results and discussion

3.1. Characterization of GLEP

The TPC of GLEP was 15.8 g/100 g gallic acid equivalents (i.e. 15.8 %). The amount of gallic acid, *Trans*-cinnamic acid, quercetin, kaempferol, hesperetin, naringenin, *p*-coumaric acid, rutin, chlorogenic acid, syringic acid, resveratrol, vanillic acid, *p*-hydroxybenzoic acid, caffeic acid, benzoic acid and catechin was 3.248 ± 0.002 μg/g, 0.164 ± 0.001 μg/g, 1.123 ± 0.013 μg/g, 1.104 ± 0.028 μg/g, 6.256 ± 0.032 μg/g, 4.854 ± 0.046 μg/g, 0.125 ± 0.001 μg/g, 0.116 ± 0.001 μg/g, 0.124 ± 0.003 μg/g, 0.101 ± 0.002 μg/g, 0.132 ± 0.006 μg/g, 0.148 ± 0.002 μg/g, 0.169 ± 0.005 μg/g, 0.102 ± 0.007 μg/g, 0.091 ± 0.006 μg/g and 0.113 μg/g, respectively. The glucans contents (total, α- and β-) was measured using Megazyme β-glucan assay kit. It was found that total glucan present in GLEP was 78.33 ± 0.04 g/100 g GLEP (i.e. 78.33 %). The amount of α-glucan was 18.18 ± 0.05 g/100 g GLEP (i.e. 18.18 %) and amount of β-glucan was 60.15 ± 2.23 g/100 g GLEP (i.e. 60.15 %).

3.2. Solubility studies

Solubility of drug in the excipients used in formulations is very important as it affects loading of the drug into the formulation. Moreover, it ensures the formation of homogenous solution rather than dispersion which, in turn, affects the size of the droplet as well as the chances of drug precipitation during storage (Savjani, Gajjar, & Savjani, 2012). Among the oils LMCS has shown maximum solubility of 95.20 ± 2.45 %, followed by CMCM (51.00 ± 3.67 %). Rest all oils have shown less than 20 % solubility of CRM. Among surfactants, CRM was maximum soluble in T80 (93.04 ± 3.45 %), followed by TP (90.23 ± 5.67 %) and Labrasol (85.50 ± 3.35 %). Based on the results of solubility studies a combination of LMCS and CMCM was used as oil. T80 and TP were used as surfactant and co-surfactants, respectively. The results of solubility studies are shown in Fig. 1.

3.3. Ternary phase diagram

A total of 81 SNEDDS prototypes were prepared (Table 1) in which the first 27 formulations (F1 to F27) were containing 1:1 ratio of CMCM and LMCS (Omix), whereas, the internal ratio of Smix was varied from 1:1 (F1 to F9), 1:2 (F10 to F18) to 2:1 (F19 to F27). Similarly, for other 27 formulations (F28 to F54), the ratio of Omix was kept 1:2 and Smix 1:1 (F28 to F36), 1:2 (F37 to F45) and 2:1 (F46 to F54). For rest of 27 formulations (F55 to F81) the ration of Omix was kept 2:1 and Smix 1:1 (F55 to F63), 1:2 (F64 to F72) and 2:1 (F73 to F81). The ternary phase for these formulations is shown in Fig. 2a–c. The results revealed that increasing the oil ratio in the composition decreased the transparency of formulation. This is caused by an increase in droplet size. This could be due to the fact that increase in oil phase increased the lipid concentration in the emulsion and the concentration of surfactants were insufficient to maintain homogeneous dispersion of nano size droplets due to increase in interfacial tension at oil-water interface. On the other hand, at decreased level of oil i.e. below 40 % and increased level of surfactants i.e. above 60 %, a decrease in interfacial tension between oil-water interface was observed which led to formation of homogeneous dispersion of nano size droplets with clear and transparent appearance (Garg et al., 2017). In Fig. 2a, nine formulations F1, F2, F3, F6, F10, F11, F12, F19 and F20 appeared as clear and transparent emulsions (indicated as SNEDDS). In Fig. 2b, seven formulations, F28, F29, F37, F39, F40, F46 and F47 showed clear and transparent appearance, whereas, in Fig. 2c, eleven formulations, F55, F56, F57, F58, F64, F65, F66, F67, F68, F73 and F74 appeared as clear and transparent emulsions. The largest SNEDDS region was observed in Fig. 2c, where the ratio of CMCM to LMCS was kept 2:1 and smallest SNEDDS region were observed for formulations that were prepared using the 1:2 ratio of CMCM and LMCS. This indicated that the concentration of CMCM played a critical role in decreasing the droplet size of SNEDDS. Similarly, among surfactant (T80) and co-surfactant (TP), the higher concentration of TP (i.e. T80: TP; 1:2) played significant role in decreasing the droplet size to nano level. It has been reported in previous studies that the interfacial fluidity of emulsions gets increased by the addition of co-surfactants as they penetrate the surfactant film and create void space between surfactant molecules. This further increases the thermodynamic stability of emulsion (Ghosh et al., 2020). These 27 SNEDDS formulations were subjected for further evaluations.

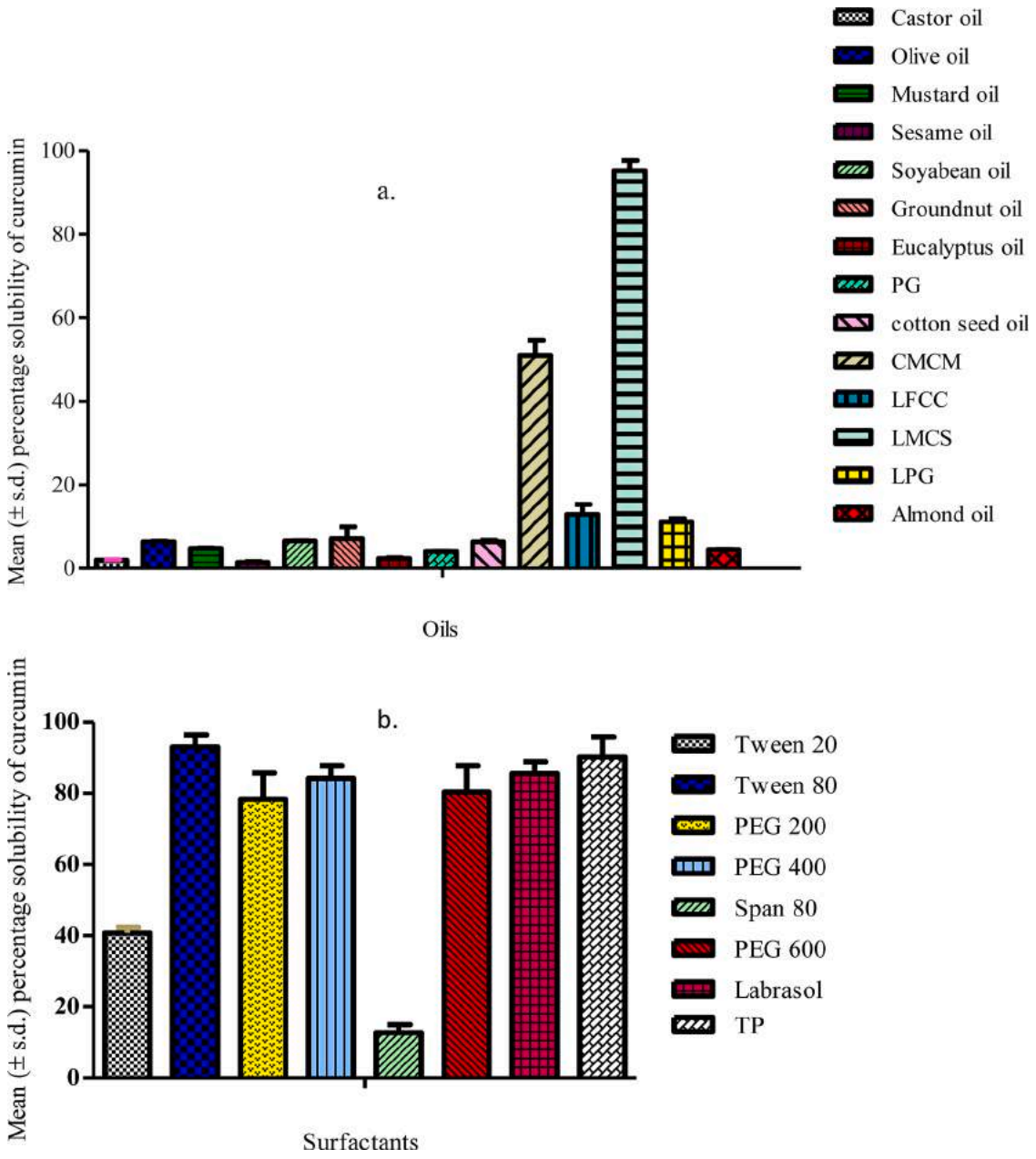

Fig. 1. Mean (± s.d.) percentage solubility of CRM in a. Oils and b. surfactants.

3.4. Determination of droplet size, drug loading and thermodynamic stability of selected L-SNEDDS

In order to optimize the best formulation with desirable deliverables, the aforementioned 27 formulations were screened for mean droplet size, drug loading (% w/w), cloud point temperature, appearance, and phase separation after storage at 40 ℃ for 48 h, centrifugation, heating /cooling cycles and after freeze/thaw cycles, respectively. The results are shown in Table 1. Their droplet size ranged from 20.22 ± 2.35 nm (F19) to 136.13 ± 1.55 nm (F57). The percentage loading of CRM in L-SNEDDS ranged from 62.80 ± 0.88 % (F28) to 98.50 ± 4.22 % (F19). The cloud point of all the 27 SNEDDS formulation was in the range of 85 to 97 ℃, indicating sufficient stability during their travel in gastrointestinal tract after getting diluted with gastric fluids (Garg et al., 2017). Absence of any phase separation or, drug precipitation during centrifugation, heating /cooling cycles and after freeze/thaw cycles indicated the stability of these formulations.

The results revealed that presence of higher amount of T80 and TP has played significant role in increasing the drug loading and decreasing the droplet size of emulsions. Moreover, it is also important to know that higher amount of T80 influenced the drug loading to a higher extent as compared to TP. As it can be seen from Table 1, the results of formulation F19 (1 mL) containing 1:9 ratio of Omix (CMCM:LMCS ratio 1:1 i.e. 5 % each) to Smix (T80:TP ratio was 2:1 i.e. T80 was 60 % and TP was 30 %) showed least droplet size, highest drug loading and better stability against thermodynamic stress and kinetic stress (centrifugation). Hence, it was selected for further characterization.

3.5. Formulation and characterization of S-SNEDDS

Formulation "F19" was subjected to solidification using various carriers. The value of L*f* for solidifying L-SNEDDS (1 g) prepared using GLEP, PB, GLEP -PB (1:1), lactose, A-200, MCC PH102 and MS was 0.71 (1.5 g), 0.67 (1.4 g), 1 (1 g), 0.43 (2.3 g), 1.25 (0.8 g), 0.77 (1.3 g) and 0.56 (1.8 g), respectively. Higher value of L*f* indicates use of less amount of carrier to convert liquid into free-flowing powder (Singh, Srinivasan,

Table 1
Composition of selected batches of CRM loaded L-SNEDDS (% w/w) and evaluation parameters (n = 3).

Formulation code	Composition for L-SNEDDS (1 mL) (CMCM: LMCS: T80:TP) (%)	Droplet size (nm) (Mean ± s.d.)	Polydispersity Index (Mean ± s.d.)	Drug Loading (%) (Mean ± s.d.)	Cloud point (℃) (Mean ± s.d.)	Appearance
F_1	5:5:45:45	43.50 ± 1.12	0.26 ± 0.06	89.81 ± 1.83	92.61 ± 2.13	TP*
F_2	10:10:40:40	68.30 ± 3.12	0.32 ± 0.04	93.23 ± 2.67	90.33 ± 1.45	TP
F_3	15:15:35:35	79.20 ± 2.11	0.36 ± 0.08	86.29 ± 1.21	89.13 ± 2.33	TP
F_6	30:30:20:20	82.70 ± 2.78	0.42 ± 0.05	84.22 ± 1.78	91.52 ± 1.56	TL**
F_{10}	50:50:30:60	28.70 ± 1.16	0.22 ± 0.09	91.20 ± 1.54	92.54 ± 3.45	TP
F_{11}	10:10:27:53	80.90 ± 2.52	0.43 ± 0.10	94.33 ± 1.84	85.27 ± 1.54	TP
F_{12}	15:15: 23:47	106.44 ± 3.04	0.45 ± 0.09	75.34 ± 1.03	88.44 ± 2.18	TL
F_{19}	5:5:60:30	20.22 ± 2.35	0.18 ± 0.02	98.50 ± 4.22	95.60 ± 3.76	TP
F_{20}	10:10:53:27	25.20 ± 2.13	0.23 ± 0.06	88.30 ± 3.54	90.87 ± 1.98	TP
F_{28}	3:7:45:45	97.20 ± 3.67	0.28 ± 0.08	62.80 ± 0.88	89.30 ± 2.56	TL
F_{29}	7:13:40:40	92.04 ± 4.11	0.30 ± 0.09	72.25 ± 2.06	91.72 ± 3.76	TL
F_{37}	3:7:30:60	59.98 ± 1.45	0.21 ± 0.03	78.62 ± 1.43	88.20 ± 1.65	TP
F_{39}	10:20: 23:47	69.56 ± 2.22	0.26 ± 0.06	85.35 ± 2.33	93.12 ± 2.54	TP
F_{40}	13:27: 20:40	120.34 ± 3.08	0.43 ± 0.09	65.71 ± 1.39	90.20 ± 3.52	TL
F_{46}	3:7:60:30	57.11 ± 0.98	0.24 ± 0.03	74.11 ± 1.65	93.50 ± 4.21	TP
F_{47}	7:13:53:27	66.09 ± 1.07	0.31 ± 0.06	82.83 ± 0.98	96.70 ± 1.94	TP
F_{55}	7:3:45:45	45.10 ± 0.88	0.35 ± 0.08	78.31 ± 0.75	89.43 ± 2.54	TP
F_{56}	13:7:40:40	122.42 ± 2.33	0.44 ± 0.05	76.92 ± 1.11	93.80 ± 3.33	TL
F_{57}	20:10: 35:35	136.13 ± 1.55	0.47 ± 0.06	65.40 ± 1.36	94.20 ± 2.45	TL
F_{58}	27:13:30:30	127.77 ± 3.11	0.41 ± 0.05	76.42 ± 2.11	95.31 ± 1.65	TL
F_{64}	7:3:30:60	69.34 ± 1.45	0.30 ± 0.02	84.31 ± 1.71	96.23 ± 3.33	TP
F_{65}	13:7: 27:53	74.33 ± 1.55	0.33 ± 0.06	69.22 ± 1.05	94.53 ± 3.54	TP
F_{66}	20:10:23:47	83.67 ± 1.09	0.29 ± 0.07	79.75 ± 1.77	90.92 ± 3.32	TP
F_{67}	27:13:20:40	38.22 ± 1.22	0.19 ± 0.02	69.91 ± 2.45	93.22 ± 2.87	TP
F_{68}	33:17:17:33	55.63 ± 1.78	0.24 ± 0.05	94.54 ± 2.74	93.54 ± 4.22	TP
F_{73}	7:3:60:30	48.11 ± 1.41	0.23 ± 0.04	73.97 ± 1.67	90.52 ± 2.56	TP
F_{74}	13:7:53:27	40.76 ± 1.52	0.20 ± 0.02	67.42 ± 1.49	91.73 ± 3.87	TP

TP* - Transparent; TL**- Translucent.

Gowthamarajan et al., 2012). A-200 has shown highest L*f* value followed by combination of synbiotics (i.e. GLEP -PB) as compared to any other carriers that have been used. It was noted that when GLEP or PB were used alone, their L*f* value was less as compared to their combination. Lactose has shown least L*f* value followed by MS. The AOR for these S-SNEDDS were found to be 27.2, 32.3, 21.8, 36.7, 19.22, 33.2, and 35.2 degrees for GLEP, PB, GLEP-PB (1:1), lactose, A-200, MCC PH102 and MS, respectively. The results indicated almost similar results of L*f* and AOR for A-200 and GLEP -PB, indicating the potential of combination of GLEP-PB to be used as carrier.

These S-SNEDDS powders were diluted in suitable solvents (as discussed in section 2.6.3.) and spray dried. These were subjected to evaluation of droplet size, zeta potential, micromeritic characteristics, percentage drug loading and thermodynamic stability studies. All the spray dried S-SNEDDS powder passed the heating-cooling cycles, freeze thaw cycles and centrifugation stress without any phase separation or, drug precipitation. The cloud point for all the spray dried S-SNEDDS powder was observed to be above 90 ℃, indicating thermodynamic stability of S-SNEDDS. The results of micromeritic properties, percentage drug loading, zeta potential and mean droplet size of all the prepared SNEDDS pre and post spray drying are shown in Table 2.

The carriers used to prepare S-SNEDDS showed high variability in their micromeritics properties. However, no significant difference ($p > 0.05$) was observed in case of drug loading and zeta potential. The mean droplet size and PDI also showed variation with respect to the carriers used. The value of flow rate was found in the range of 0.88 g/s (Lactose) to 3.16 g/s (A-200). The AOR was found in the range of 19.22°Θ (A-200) to 36.70°Θ (Lactose). TD was found in the range of 1.25 g/cm^3 (GLEP -PB) to 1.82 g/cm^3 (Lactose). Similarly, BD was found in the range of 0.275 g/cm^3 (A-200) to 0.357 g/cm^3 (Lactose) and TPD was found in the range of 0.396 g/cm^3 (A-200) to 0.510 g/cm^3 (PB). The CCI was found in the range of 25.0 (Lactose) to 38.74 (MCC PH 102). These differences in the micromeritics properties of various carriers can be attributed to differences in their physicochemical properties and loading factor. A-200 showed very good flow rate, TP, BD and TPD as compared to other solid carriers used, owing to its fluffy nature and higher surface area (Beg et al., 2016). In contrast, least flow rate and higher density values were obtained in case of lactose. The S-SNEDDS prepared using GLEP-PB as carrier also showed good flow rate and density values following A-200. This indicated that S-SNEDDS prepared using GLEP-PB as carrier possessed almost comparable flow behaviour as that of S-SNEDDS prepared using A-200, which is the most acceptable carrier used to solidify S-SNEDDS (B. Singh et al., 2009). However, the major advantage of using GLEP-PB as solid carrier was its CCI value. The CCI value of GLEP-PB was found to be comparatively less as compared to the CCI value of A-200. Lesser value of CCI indicated very good compaction properties of the carrier (Beg et al., 2016). Furthermore, the least mean droplet size and highest zeta potential was observed for the S-SNEDDS prepared using GLEP-PB as carrier. The polysaccharides present in GLEP, provide more negative charge to the formulation and shifted the zeta potential towards more negative side, indicating better adsorption of emulsion on the carrier (Kumari et al., 2020). All the properties got improved upon spray dying except droplet size. The micromeritics properties got improved upon spray drying due to removal of moisture from S-SNEDDS powders and better adsorption of L-SNEDDS during their cyclonic drying in the chamber of spray dryer. The shift of zeta potential towards higher value can be ascribed to better surface adsorption of L-SNEDDS in the matrix of solid carrier and based upon the extent of negative charge present in the carrier they shifted the zeta potential. It is important to note that shifting of zeta potential towards higher sides indicates better stability of formulation (Kumar Singh et al., 2016). The increase in droplet size upon solidification is due to the dispersion of liquid droplets and solid carrier in aqueous medium. The carrier that provided better solubility in the aqueous medium showed a clear transparent emulsion upon dilution followed by the one which had lesser solubility in the medium. Upon spray drying the size of the droplets further got increased due to higher adherence/adsorption of liquid droplets with their solid carriers (B. K. Kang et al., 2004; B. Kumar et al., 2018). The drug loading of all the formulation was found to be above 95%. Hence, based on overall performance of S-SNEDDS prepared using GLEP-PB as carrier i.e. high flow rate, low CCI value, good angle of repose, good drug loading, high zeta potential and least droplet size, it

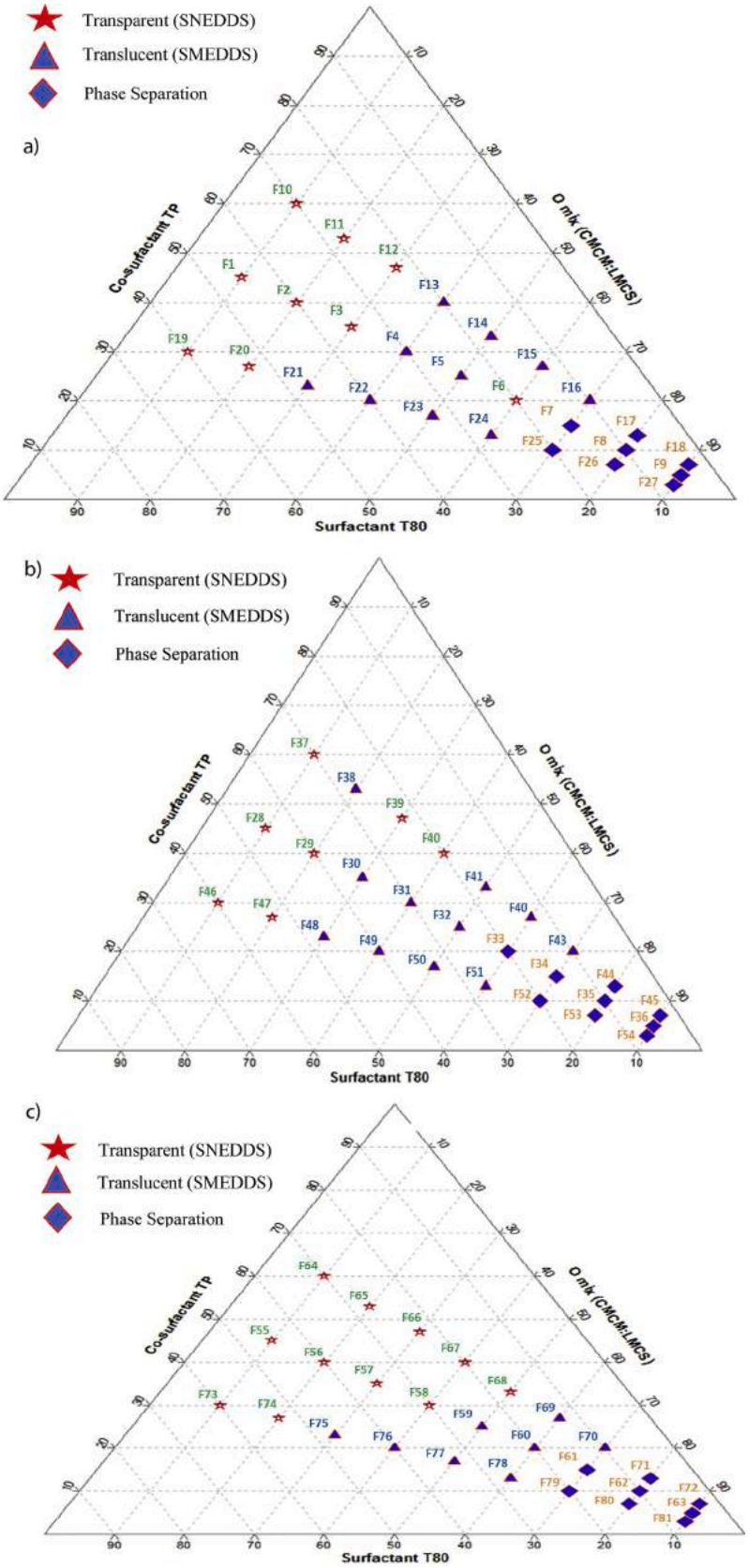

Fig. 2. Ternary phase diagram for 81 SNEDDS prototypes a. F1-F27; b. F28-F54; c. F55-F81.

Table 2
Mean (±s.d.) results of micromeritic characteristics, droplet size, zeta potential and percentage drug loading of S-SNEDDS (n = 3).

Component	Flow rate (g/s)	Angle of repose (Θ)	True Density (g/cm^3)	Bulk Density (g/cm^3)	Tap Density (g/cm^3)	CCI	Drug loading (%)	Mean droplet size (nm)	PDI	Zeta Potential (mV)
L-SNEDDS (F19)	NA	NA	NA	NA	NA	NA	98.50 ± 4.22	20.22 ± 2.35	0.18 ± 0.02	−19.2 ± 0.16
S-SNEDDS (F19)		**Prior to spray drying**								
A-200	3.16 ± 0.34	19.22 ± 1.33	1.46 ± 0.34	0.275 ± 0.02	0.396 ± 0.02	30.55 ± 3.04	96.84 ± 3.18	40.45 ± 1.78	0.23 ± 0.05	−16.96 ± 1.15
GLEP	2.84 ± 0.18	29.20 ± 2.18	1.52 ± 0.22	0.320 ± 0.05	0.476 ± 0.05	32.77 ± 2.06	96.65 ± 2.45	32.28 ± 2.56	0.21 ± 0.08	−17.84 ± 1.75
PB	1.95 ± 0.22	32.30 ± 3.21	1.68 ± 0.19	0.336 ± 0.04	0.510 ± 0.07	34.12 ± 2.15	97.13 ± 3.24	46.78 ± 3.18	0.26 ± 0.03	−18.22 ± 3.25
GLEP-PB (1:1)	3.10 ± 0.23	23.80 ± 2.16	1.25 ± 0.18	0.310 ± 0.03	0.415 ± 0.05	25.31 ± 2.04	98.12 ± 3.43	28.50 ± 1.43	0.16 ± 0.01	- 22.10 ± 0.22
MCC PH102	2.10 ± 0.33	33.24 ± 2.17	1.60 ± 0.22	0.310 ± 0.01	0.506 ± 0.22	38.74 ± 3.09	96.88 ± 4.19	54.18 ± 3.12	0.31 ± 0.08	- 18.22 ± 0.34
MS	0.91 ± 0.10	35.20 ± 1.88	1.50 ± 0.37	0.296 ± 0.09	0.435 ± 0.09	31.95 ± 2.22	± 3.12	78.22 ± 3.65	0.33 ± 0.06	- 15.23 ± 0.44
Lactose	0.88 ± 0.18	36.70 ± 2.56	1.82 ± 0.45	0.357 ± 0.05	0.476 ± 0.02	25.00 ± 1.85	96.34 ± 3.21	81.34 ± 2.59	0.36 ± 0.08	- 16.17 ± 0.78
S-SNEDDS (F19)		**Post spray drying**								
A-200	4.18 ± 0.56	16.34 ± 2.10	1.32 ± 0.26	0.260 ± 0.07	0.361 ± 0.05	27.98 ± 2.89	95.22 ± 4.16	52.22 ± 2.38	0.18 ± 0.05	−17.58 ± 2.23
GLEP	3.22 ± 0.18	25.33 ± 3.22	1.41 ± 0.32	0.302 ± 0.06	0.412 ± 0.08	26.69 ± 0.87	95.62 ± 3.22	42.20 ± 5.88	0.16 ± 0.02	−18.78 ± 3.32
PB	2.59 ± 0.33	28.22 ± 1.56	1.48 ± 0.28	0.312 ± 0.03	0.455 ± 0.09	31.43 ± 1.34	96.22 ± 5.10	58.68 ± 4.21	0.12 ± 0.04	−19.23 ± 2.10
GLEP-PB (1:1)	3.89 ± 0.55	20.31 ± 3.22	1.18 ± 0.31	0.296 ± 0.02	0.368 ± 0.06	19.56 ± 2.67	96.81 ± 4.32	35.22 ± 2.34	0.15 ± 0.03	- 23.22 ± 1.48
MCC PH102	2.81 ± 0.18	32.36 ± 3.48	1.54 ± 0.22	0.293 ± 0.05	0.454 ± 0.08	35.46 ± 1.25	96.88 ± 4.19	72.59 ± 3.10	0.28 ± 0.03	- 18.36 ± 2.12
MS	1.30 ± 0.19	34.72 ± 3.17	1.38 ± 0.25	0.272 ± 0.09	0.410 ± 0.09	33.66 ± 1.56	95.22 ± 2.87	96.18 ± 4.55	0.30 ± 0.09	- 16.18 ± 1.15
Lactose	1.10 ± 0.89	35.67 ± 4.52	1.70 ± 0.33	0.330 ± 0.10	0.428 ± 0.15	22.90 ± 1.22	94.95 ± 4.98	112.20 ± 4.98	0.40 ± 0.03	- 17.32 ± 1.23

was considered as an optimum carrier to solidify emulsions. The survival rate for *Bacillus mesentericus, Clostridium butyricum, Lactobacillus acidophilus and Streptococcus thermophilus* was found to be 75.22 ± 2.22 %, 78.34 ± 3.87 %, 72.38 ± 2.26 %, and 68.54 ± 4.35 %, respectively. It is important to note that there are several reports where excellent survival rate of bacteriae present in probiotics has been reported at an outlet temperature of 85-90 ℃ (Ananta & Knorr, 2003; G. Gardiner et al., 2000; G. E. Gardiner et al., 2002; Kim & Bhowmik, 1990; Simpson, Stanton, Fitzgerald, & Ross, 2005).

The spray dried S-SNEDDS powders prepared using GLEP-PB as solid carrier were further subjected to extrusion-spheronization for formulating spheroids. The prepared spheroids showed flow rate of 5.12 ± 0.76 g/s, 18.26 ± 1.38°Θ AOR, 0.218 ± 0.05 g/cm^3 BD, 0.263 ± 0.04 g/cm^3 TPD, 17.11 ± 2.18 CCI, 95.64 ± 3.21 % drug loading, 37.64 ± 2.56 nm mean droplet size, 0.16 ± 0.03 PDI and -21.48 ± 2.18 mV zeta potential. It is important to note that an increase in mean droplet size was observed when the L-SNEDDS (20.22 ± 2.35 nm) were converted to S-SNEDDS powder using GLEP-PB (1:1) as carrier (35.22 ± 2.34 nm) and spheroids (37.64 ± 2.56 nm). However, their p values were found to be above 0.05 indicating no significant change upon their transformation from powder form to spheroids. The p value between L-SNEDDS and GLEP-PB-S-SNEDDS powder was 0.251. Similarly, it was 0.156 between L-SNEDDS and GLEP-PB-S-SNEDDS spheroids. No significant change ($p > 0.05$) was observed in case of % drug loading and zeta potential upon transformation of L-SNEDDS into S-SNEDDS powder and S-SNEDDS spheroids.

3.6. DSC analysis

CRM showed a sharp crystalline endothermic peak at 172 ℃, whereas, the excipients used in the formulation (GLEP, PB, A-200, CMCM, LMCS, T80, and TP) showed amorphous nature as depicted by their halo pattern with absence of any sharp peaks. The S-SNEDDS formulations (non-spray dried and spray dried powder as well as spheroids) also showed amorphous halo pattern indicating complete solubility of drug in the liquid formulation and adsorption of liquid onto the porous surface of synbiotics. The results are shown in Fig. 3.

3.7. PXRD analysis

The PXRD pattern of raw CRM, PB, GLEP, A-200, and GLEP-PB-S-SNEDDS powder (spray and non spray dried) was recorded and results are shown in Fig. 4. CRM showed crystalline nature, whereas, A-200 and GLEP showed amorphous nature. PB showed some sharp peaks followed by halo pattern (absence of peaks) indicating its semi-crystalline nature. Similar results of DSC, PXRD results also indicated amorphous nature of S-SNEDDS formulations (halo pattern) indicating complete solubility of crystalline drug in the liquid formulation. It is important to note that the amorphous nature of formulations got enhanced after spray drying (Fig. 4f) due to uniform mixing of porous carriers and L-SNEDDS pre-concentrate that allowed complete adsorption of dissolved CRM on carriers' surface (B. K. Kang et al., 2004; B. Kumar et al., 2018; Sharma et al., 2018).

3.8. Microscopic analysis

The TEM images of L-SNEDDS (Fig. 5a) and GLEP-PB-S-SNEDDS (spray dried) (Fig. 5b) revealed spherical and unagglomerated droplets in nanometer size range. The mean droplet size of L-SNEDDS and GLEP-PB-S-SNEDDS (spray dried) obtained through dynamic light scattering were 20.22 ± 2.35 nm and 35.22 ± 2.34 nm, respectively (Table 2). The results of TEM also indicated the mean size of droplets for

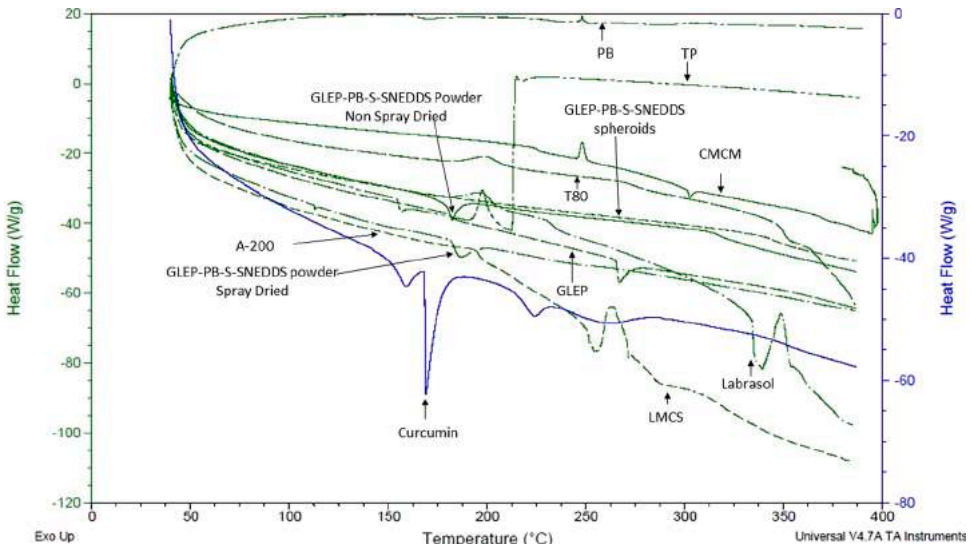

Fig. 3. DSC thermograms of curcumin, excipients as well as S-SNEDDS formulations.

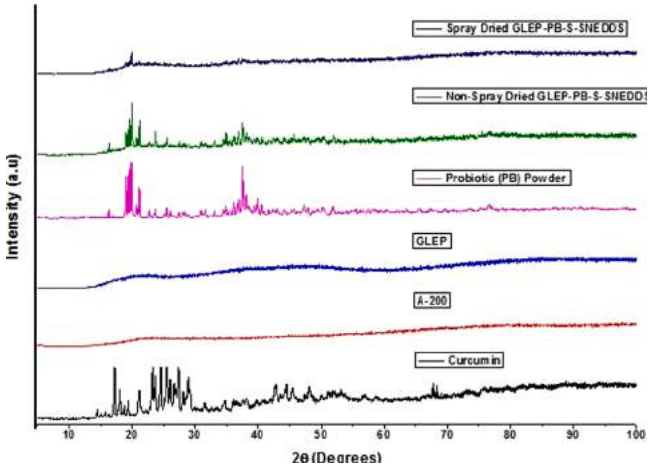

Fig. 4. Overlay of PXRD patterns of curcumin, PB; GLEP, A-200, GLEP-PB-S-SNEDDS non-spray dried powder and GLEP-PB-S-SNEDDS spray dried powder.

both the formulations to be less than 50 nm [i.e. 26.21 ± 3.32 nm for L-SNEDDS and 33.18 ± 2.28 nm GLEP-PB-S-SNEDDS (spray dried)].

The SEM images of raw CRM, PB, GLEP, A-200, and GLEP-PB-S-SNEDDS powder (spray and non spray dried) are shown in Fig. 6a–f. CRM showed long blade like crystalline structure with sharp edges (Fig.6a). The structure of GLEP appeared as long, striated, rectangular structure with porous and rough reticulated surface (Fig. 6b). The structure of PB was found as long with porous and rough surface and irregular and reticulated edges (Fig. 6c). A-200 was found to have highly porous and smooth surface indicating its amorphous nature (Fig. 6d). The GLEP-PB-S-SNEDDS powder (non spray dried) appeared as rough-surfaced particles with porous and waxy appearance indicating the presence of adsorbed liquid SNEDDS preconcentrate on the porous surface of carriers, particularly GLEP and A-200 (Fig. 6e). Upon spray drying, the particles looked smooth, porous and spherical with absence of any waxy appearance indicating complete adsorption of liquid SNEDDS preconcentrate on surface of carriers (Fig. 6f). Thus, the obtained results were found similar to the observations obtained for developed S-SNEDDS formulation as that of PXRD and DSC studies. Moreover, the obtained results of SEM for S-SNEDDS formulations have justified better micromeritic properties for S-SNEDDS after drying as compared to that of non-spray dried powder (as shown in Table 2). Spray drying of S-SNEDDS provided better interaction between liquids and the porous carriers during the drying process. Moreover, during drying, the moisture present in the solid carriers also gets dried and provides better void spaces for adsorption of liquid preconcentrate. The overall result is an un-agglomerated, porous-sponge like, spherical and

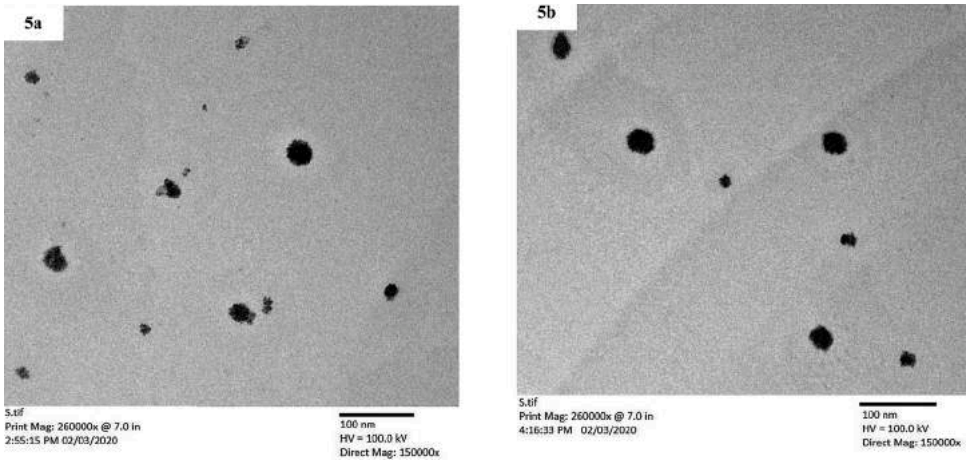

Fig. 5. TEM images of a. L-SNEDDS and b. GLEP-PB-S-SNEDDS (spray dried).

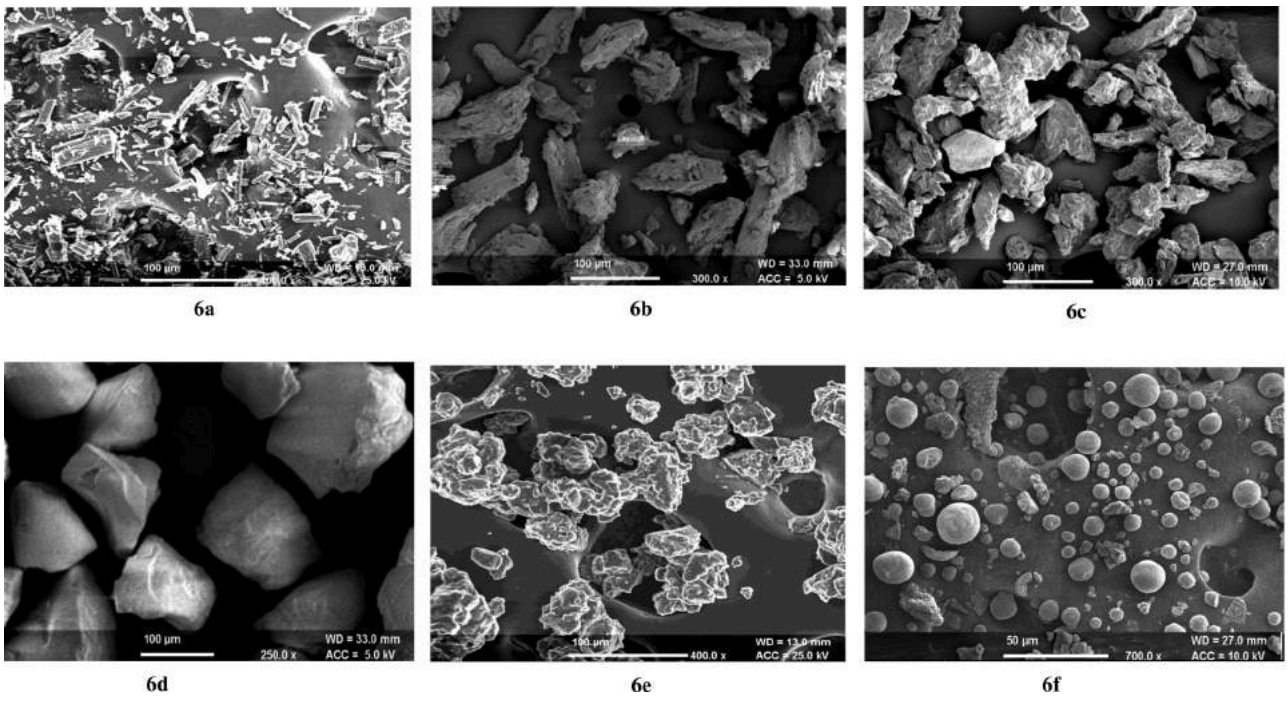

Fig. 6. SEM images of a. raw CRM; b. GLEP; c. PB; d. A-200; e. GLEP-PB-S-SNEDDS (non spray dried) powder; f. GLEP-PB-S-SNEDDS (spray dried) powder.

free flowing S-SNEDDS powder that can be easily stored in any container/capsules as such or, can be converted into convenient solid dosage forms such as tablets or, spheroids. Similar observations were noted in previous studies also when the liquid SNEDDS have been spray dried (Beg et al., 2016; B. K. Kang et al., 2004; B. Kumar et al., 2018; Rajesh et al., 2018; Sharma et al., 2018).

3.9. Effect of pH and dilution on emulsion droplet size

The results (Fig. 7a) showed negligible increase in droplet size with increase in pH of the medium and decrease in the dilution of the medium. The significance of performing this study was to understand the fate of formulation upon its oral administration as the pH and volume of medium varies throughout GIT. The non-significant ($p > 0.05$) change in the droplet size with variation in pH and dilution indicated about stability of the GLEP-PB-S-SNEDDS upon their oral administration.

3.10. In vitro cell line permeability studies

This study was performed to evaluate the transport of CRM across the intestinal membrane through various SNEDDS formulation. As presented in Fig. 7b, it was observed that L-SNEDDS exhibited 4.15 folds higher permeation of CRM (A-B) as compared to the unprocessed CRM, and 0.91 folds lower drug excretion (B-A) than unprocessed CRM at 5 h. The permeation of CRM was found to be 3.55 and 3.15 folds higher from GLEP-PB-S-SNEDDS powder and GLEP-PB-S-SNEDDS spheroids as compared to its unprocessed form. The p value for drug's permeation between unprocessed CRM and L-SNEDDS was 0.017 and it was 0.023 between unprocessed CRM and GLEP-PB-S-SNEDDS powder. Similarly, p value for drug's permeation between unprocessed CRM and GLEP-PB-S-SNEDDS spheroids was 0.034. All these values were found to be less than 0.05, indicating significant enhancement in drug's permeation by loading CRM into SNEDDS as that of its unprocessed form. The p value between L-SNEDDS and GLEP-PB-S-SNEDDS powder, L-SNEDDS and GLEP-PB-S-SNEDDS spheroids and GLEP-PB-S-SNEDDS powder and GLEP-PB-S-SNEDDS spheroids was 0.168, 0.105, and 0.213, respectively. All these values were above 0.05, indicating non-significant difference in drug's permeation through all the SNEDDS formulation. A number of studies have demonstrated the ability of SNEDDS to improve the intestinal lymphatic transport of the hydrophobic drugs (Date, Desai, Dixit, & Nagarsenker, 2010). Our study also proves that transportation of BCS class IV drug (CRM) is facilitated by formulating it in the form of SNEDDS.

3.11. Dissolution study

The *in vitro* dissolution study revealed more than 90 percent drug release within first 5 min from L-SNEDDS, GLEP-PB-S-SNEDDS powder and its spheroids whereas, only 20 percent drug release was observed from the unprocessed CRM (Fig. 8a). This indicated that the dissolution rate of CRM got enhanced by 4.5 folds by loading it into SNEDDS due to complete solubility of drug in the emulsion. The release profiles of unprocessed CRM, L-SNEDDS and S-SNEDDS were compared using one-way ANOVA and f2 value. The p-value was found to be less than 0.0001 and f2 value less than 50 between unprocessed CRM and all SNEDDS formulations indicating significant improvement in drug's release upon converting into SNEDDS (Shah et al., 1998). The p-values between L-SNEDDS and GLEP-PB-S-SNEDDS powder, L-SNEDDS and GLEP-PB-S-SNEDDS spheroids and GLEP-PB-S-SNEDDS powder and GLEP-PB-S-SNEDDS spheroids were found to be above 0.45. The f2 value between L-SNEDDS and GLEP-PB-S-SNEDDS powder, L-SNEDDS and GLEP-PB-S-SNEDDS spheroids and GLEP-PB-S-SNEDDS powder and GLEP-PB-S-SNEDDS spheroids were found to be 69.89, 51.67 and 62.93, respectively. The p-values above 0.05 and f2 values above 50 indicated non-significant change in results which ultimately proved that solidification of liquid SNEDDS and its further conversion into spheroids did not retard the dissolution profile of CRM. Higher permeability and higher dissolution rates are indicative of higher bioavailability of lipophilic drugs upon their oral administration because permeation of drug is directly proportional to availability of drug in systemic circulation (R. Kumar et al., 2019).

3.12. Stability studies

The mean droplet size of aged GLEP-PB-S-SNEDDS powder and its spheroids were found to be 40.22 ± 2.56 nm and 45.71 ± 1.81 nm

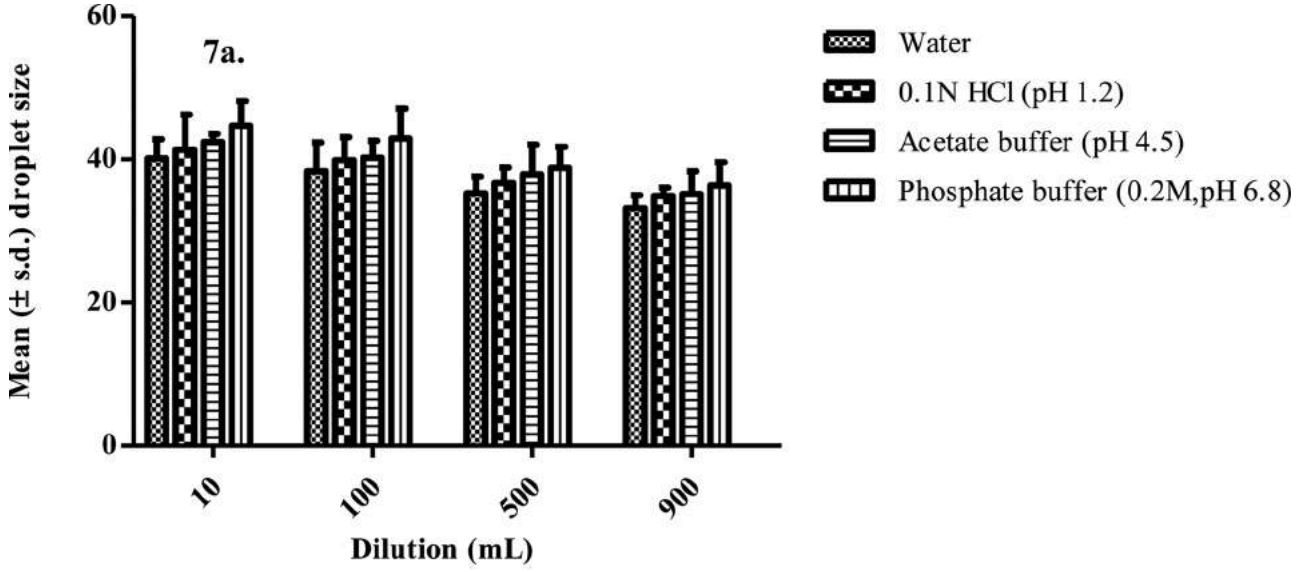

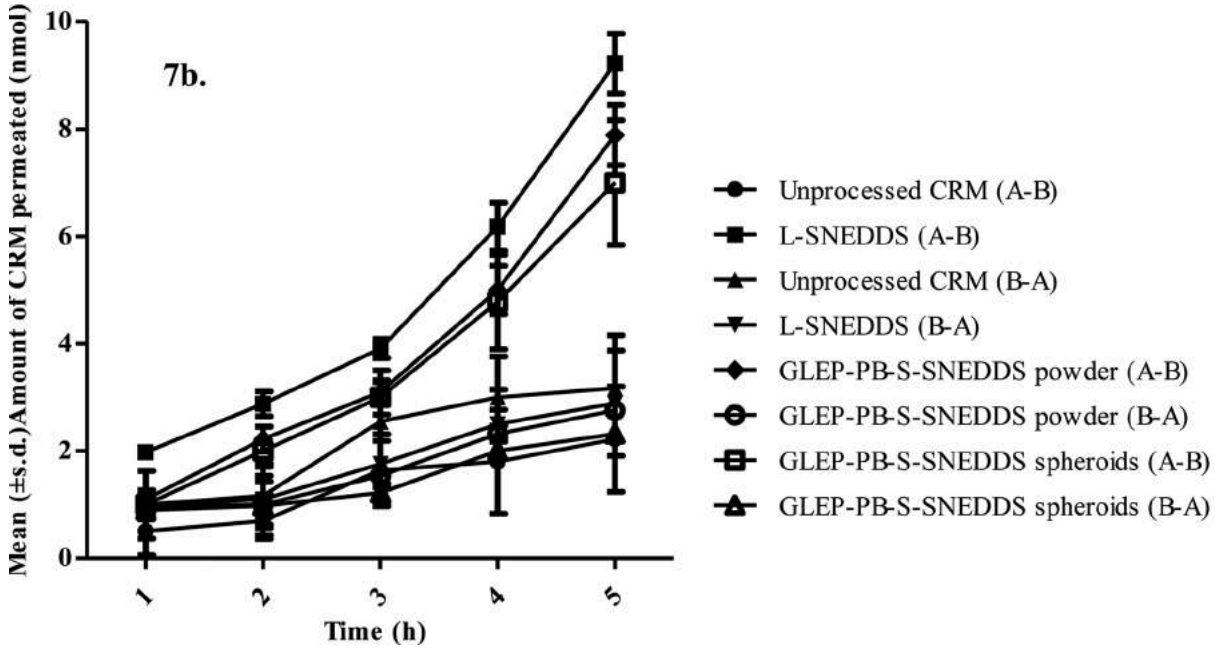

Fig. 7. a. Results of effect of dilution and pH change on mean droplet size (n = 3); **b.** *In vitro* transport study of unprocessed CRM and its SNEDDS formulations through caco2 cell lines (n = 3).

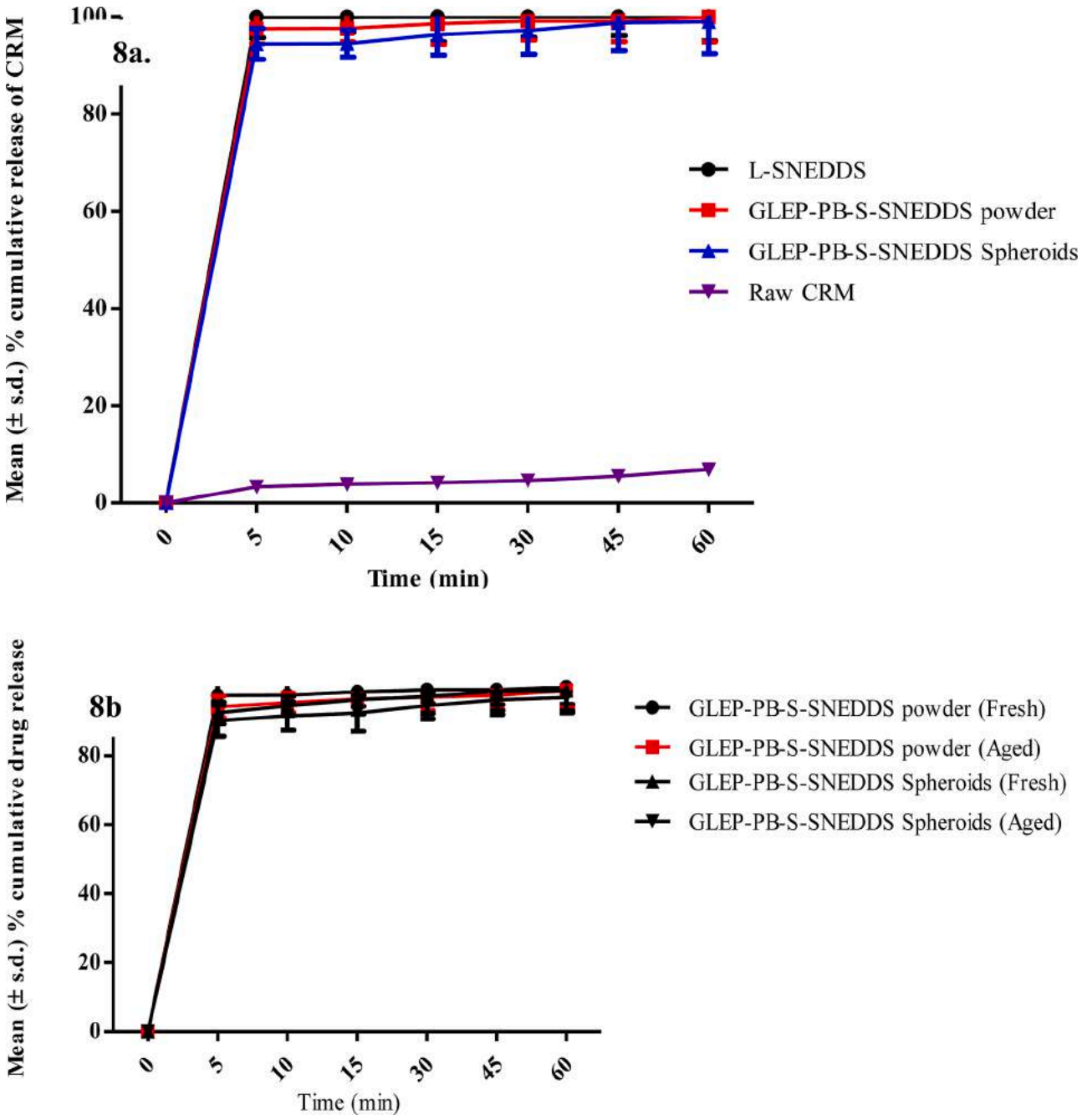

Fig. 8. a. Results of mean (± s.d.) percentage cumulative release of unprocessed CRM and its SNEDDS formulations (n = 6); b. Mean (± s.d.) percentage cumulative release of aged and fresh S-SNEDDS formulations (n = 6).

respectively, while, the droplet size of fresh S-SNEDDS formulations was 35.22 ± 2.34 nm (GLEP-PB-S-SNEDDS powder) and 37.64 ± 2.56 nm (GLEP-PB-S-SNEDDS spheroids) respectively. Similarly, the drug loading for fresh S-SNEDDS was 96.81 ± 4.32 % (GLEP-PB-S-SNEDDS powder) and 95.64 ± 3.21 % (GLEP-PB-S-SNEDDS spheroids) and for aged S-SNEDDS, it was 94.61 ± 3.34 % (GLEP-PB-S-SNEDDS powder) and 92.58 ± 1.18 % (GLEP-PB-S-SNEDDS spheroids). The AOR for fresh S-SNEDDS was 20.31 ± 3.22°Θ (GLEP-PB-S-SNEDDS powder) and 18.26 ± 1.38°Θ (GLEP-PB-S-SNEDDS spheroids) and for aged S-SNEDDS, it was 25.22 ± 3.26°Θ (GLEP-PB-S-SNEDDS powder) and 21.54 ± 2.45°Θ (GLEP-PB-S-SNEDDS spheroids). A non-significant difference ($p > 0.05$) in aforementioned results indicated that the prepared formulations were stable. Similar non-significant difference was observed in the dissolution profiles of aged and fresh formulations. In all the cases more than 90 percentage drug got released from the formulation (Fig. 8b). The f2 value was found to be 63.20 and 57.94 for aged and fresh S-SNEDDS powder and spheroids indicated similar dissolution profiles (Shah et al., 1998).

4. Conclusion

The study entailed successful development of CRM loaded self-nanoemulsifying formulation to enhance the dissolution rate and permeability of lipophilic CRM. Synbiotics (GLEP-PB) proved to be efficient solid carriers to solidify L-SNEDDS as they were able to provide good adsorption property, AOR, CCI, flow rate, drug loading, droplet size and zeta potential. Furthermore, the non-significant difference in mean droplet size, drug loading, zeta potential, drug permeation and

dissolution behaviour of CRM loaded in L-SNEDDS and S-SNEDDS (both powder and spheroids) indicate towards successful transformation of liquid SNEDDS into solid form without alteration in product's performance. The successful formulation of S-SNEDDS powder into spheroids indicated excellent compaction property of GLEP-PB. Absence in any significant difference between aged and fresh formulations indicated the potential of GLEP-PB to provide stable formulations. In a nutshell, looking on aforementioned properties of GLEP-PB, it can be further explored to solidify other lipid-based delivery systems.

CRediT authorship contribution statement

Rubiya Khursheed: Methodology, Data curation, Writing - original draft. **Sachin Kumar Singh:** Conceptualization, Validation, Supervision, Writing - review & editing. **Sheetu Wadhwa:** Supervision. **Monica Gulati:** Supervision, Writing - review & editing. **Ankit Awasthi:** Methodology. **Rajan Kumar:** Methodology, Data curation. **Arya Kadukkattil Ramanunny:** Methodology. **Bhupinder Kapoor:** Methodology. **Pushpendra Kumar:** Methodology. **Leander Corrie:** Methodology.

Declaration of Competing Interest

The authors report no declarations of interest.

Appendix A. Supplementary data

Supplementary material related to this article can be found, in the online version, at doi:https://doi.org/10.1016/j.carbpol.2020.116996.

References

Ahir, A. A., Mali, S. S., Hajare, A. A., Bhagwat, D. A., & Patrekar, P. V. (2015). Pelletization technology: Methods and applications-A review. *Research Journal of Pharmacy and Technology, 8*(2), 131–138.

Ananta, E., & Knorr, D. (2003). Pressure-induced thermotolerance of Lactobacillus rhamnosus GG. *Food research international, 36*(9-10), 991–997.

Beg, S., Katare, O., Saini, S., Garg, B., Khurana, R. K., & Singh, B. (2016). Solid self-nanoemulsifying systems of olmesartan medoxomil: Formulation development, micromeritic characterization, in vitro and in vivo evaluation. *Powder Technology, 294*, 93–104.

Brown, C. K., Chokshi, H. P., Nickerson, B., Reed, R. A., Rohrs, B. R., & Shah, P. A. (2004). Dissolution testing of poorly soluble compounds. *Pharm. Tech, 28*, 56-43.

Danki, L. S., & Thube, S. S. (2010). Studies on the Effect of Ternary Complex Formation of Simvastatin: β-Cyclodextrin with Polyvinyl Pyrrolidone and Hydroxypropyl Methylcellulose. *Research Journal of Pharmacy and Technology, 3*(4), 1148–1151.

Date, A. A., Desai, N., Dixit, R., & Nagarsenker, M. (2010). Self-nanoemulsifying drug delivery systems: formulation insights, applications and advances. *Nanomedicine, 5*(10), 1595–1616.

Deb, R., & Ahmed, A. (2013). Pellets and Pelletization techniques: A critical review. *Int Res J Pharm, 4*(4), 90–95.

Gardiner, G., O'sullivan, E., Kelly, J., Auty, M., Fitzgerald, G., Collins, J., & Stanton, C. (2000). Comparative survival rates of human-derived probioticlactobacillus paracasei and l. salivariusstrains during heat treatment and spray drying. *Applied and environmental microbiology, 66*(6), 2605–2612.

Gardiner, G. E., Bouchier, P., O'Sullivan, E., Kelly, J., Collins, J. K., Fitzgerald, G., & Stanton, C. (2002). A spray-dried culture for probiotic Cheddar cheese manufacture. *International Dairy Journal, 12*(9), 749–756.

Garg, V., Kaur, P., Gulati, M., Singh, S. K., Kumar, B., Pandey, N. K., & De, A. (2019). Coadministration of Polypeptide-k and Curcumin Through Solid Self-Nanoemulsifying Drug Delivery System for Better Therapeutic Effect Against Diabetes Mellitus: Formulation, Optimization, Biopharmaceutical Characterization, and Pharmacodynamic Assessment. *Assay and drug development technologies*.

Garg, V., Kaur, P., Singh, S. K., Kumar, B., Bawa, P., Gulati, M., … Yadav, A. K. (2017). Solid self-nanoemulsifying drug delivery systems for oral delivery of polypeptide-k: Formulation, optimization, in-vitro and in-vivo antidiabetic evaluation. *European Journal of Pharmaceutical Sciences, 109*, 297–315.

Ghai, D., & Sinha, V. R. (2012). Nanoemulsions as self-emulsified drug delivery carriers for enhanced permeability of the poorly water-soluble selective β1-adrenoreceptor blocker Talinolol. *Nanomedicine: Nanotechnology, Biology and Medicine, 8*(5), 618–626.

Ghosh, D., Singh, S. K., Khursheed, R., Pandey, N. K., Kumar, B., Kumar, R., & Awasthi, A. (2020). Impact of solidification on micromeritic properties and dissolution rate of self-nanoemulsifying delivery system loaded with docosahexaenoic acid. *Drug development and industrial pharmacy*, 1–33 (just-accepted).

Gowthamarajan, K., & Singh, S. K. (2010). Dissolution testing for poorly soluble drugs: a continuing perspective. *Dissolution Technologies, 17*(3), 24–32.

Hur, K. Y., & Lee, M.-S. (2015). Gut microbiota and metabolic disorders. *Diabetes Metabolism Journal, 39*(3), 198–203.

Inugala, S., Eedara, B. B., Sunkavalli, S., Dhurke, R., Kandadi, P., Jukanti, R., … Bandari, S. (2015). Solid self-nanoemulsifying drug delivery system (S-SNEDDS) of darunavir for improved dissolution and oral bioavailability: in vitro and in vivo evaluation. *European Journal of Pharmaceutical Sciences, 74*, 1–10.

Jeong, S. C., Jeong, Y. T., Yang, B. K., Islam, R., Koyyalamudi, S. R., Pang, G., & Song, C. H. (2010). White button mushroom (Agaricus bisporus) lowers blood glucose and cholesterol levels in diabetic and hypercholesterolemic rats. *Nutrition research, 30*(1), 49–56.

Jyoti, J., Anandhakrishnan, N. K., Singh, S. K., Kumar, B., Gulati, M., Gowthamarajan, K., & Pandey, N. K. (2019). A three-pronged formulation approach to improve oral bioavailability and therapeutic efficacy of two lipophilic drugs with gastric lability. *Drug delivery and translational research, 9*(4), 848–865.

Kallakunta, V. R., Bandari, S., Jukanti, R., & Veerareddy, P. R. (2012). Oral self emulsifying powder of lercanidipine hydrochloride: formulation and evaluation. *Powder Technology, 221*, 375–382.

Kamel, A. O., & Mahmoud, A. A. (2013). Enhancement of human oral bioavailability and in vitro antitumor activity of rosuvastatin via spray dried self-nanoemulsifying drug delivery system. *Journal of biomedical nanotechnology, 9*(1), 26–39.

Kang, B. K., Lee, J. S., Chon, S. K., Jeong, S. Y., Yuk, S. H., Khang, G., & Cho, S. H. (2004). Development of self-microemulsifying drug delivery systems (SMEDDS) for oral bioavailability enhancement of simvastatin in beagle dogs. *International journal of pharmaceutics, 274*(1-2), 65–73.

Kang, J. H., Oh, D. H., Oh, Y.-K., Yong, C. S., & Choi, H.-G. (2012). Effects of solid carriers on the crystalline properties, dissolution and bioavailability of flurbiprofen in solid self-nanoemulsifying drug delivery system (solid SNEDDS). *European Journal of Pharmaceutics and Biopharmaceutics, 80*(2), 289–297.

Kaur, P., Singh, S. K., Garg, V., Gulati, M., & Vaidya, Y. (2015). Optimization of spray drying process for formulation of solid dispersion containing polypeptide-k powder through quality by design approach. *Powder Technology, 284*, 1–11.

Kazi, M., Al-Swairi, M., Ahmad, A., Raish, M., Alanazi, F. K., Khan, A. A., & Hussain, M. D. (2019). Evaluation of self-nanoemulsifying drug delivery system (SNEDDS) for poorly water-soluble talinolol: preparation, in vitro and in vivo assessment. *Frontiers in pharmacology, 10*, 459.

Khan, A. W., Kotta, S., Ansari, S. H., Sharma, R. K., & Ali, J. (2015). Self-nanoemulsifying drug delivery system (SNEDDS) of the poorly water-soluble grapefruit flavonoid Naringenin: design, characterization, in vitro and in vivo evaluation. *Drug delivery, 22*(4), 552–561.

Khan, I., Huang, G., Li, X., Leong, W., Xia, & Hsiao, W. L. W. (2018). Mushroom polysaccharides from Ganoderma lucidum and Poria cocos reveal prebiotic functions. *Journal of Functional Foods, 41*, 191–201.

Khanna, P. (2011). Polysaccharides from medicinal mushrooms and their antitumor activities-A review. *International Journal of Food and Fermentation Technology, 1*(1), 17–37.

Khursheed, R., Singh, S. K., Wadhwa, S., Kapoor, B., Gulati, M., Kumar, R., & Dua, K. (2019). Treatment strategies against diabetes: Success so far and challenges ahead. *European journal of pharmacology*, Article 172625.

Khursheed, R., Singh, S. K., Wadhwa, S., Gulati, M., & Awasthi, A. (2020). Therapeutic potential of mushrooms in diabetes mellitus: Role of polysaccharides. *International Journal of Biological Macromolecules, 164*, 1194–1205.

Kim, S. S., & Bhowmik, S. R. (1990). Survival of lactic acid bacteria during spray drying of plain yogurt. *Journal of food science, 55*(4), 1008–1010.

Kozarski, M., Klaus, A., Nikšić, M., et al. (2012). Antioxidative activities and chemical characterization of polysaccharide extracts from widely used mushrooms Ganoderma applanatum, Ganoderma lucidum, Lentinus edodes and Trametes versicolor. *Journal of Food Composition and Analysis, 26*, 144–153.

Kumar, B., Garg, V., Singh, S., Pandey, N. K., Bhatia, A., Prakash, T., & Singh, S. K. (2018). Impact of spray drying over conventional surface adsorption technique for improvement in micromeritic and biopharmaceutical characteristics of self-nanoemulsifying powder loaded with two lipophilic as well as gastrointestinal labile drugs. *Powder Technology, 326*, 425–442.

Kumar, R., Khursheed, R., Kumar, R., Awasthi, A., Sharma, N., Khurana, S., & Gowthamarajan, K. (2019). Self-nanoemulsifying drug delivery system of fisetin: Formulation, optimization, characterization and cytotoxicity assessment. *Journal of Drug Delivery Science and Technology, 54*, Article 101252.

Kumar Singh, S., Vaidya, Y., Gulati, M., Bhattacharya, S., Garg, V., & Kumar Pandey, N. (2016). Nanosuspension: principles, perspectives and practices. *Current drug delivery, 13*(8), 1222–1246.

Kumar, V. V., Chandrasekar, D., Ramakrishna, S., Kishan, V., Rao, Y. M., & Diwan, P. V. (2007). Development and evaluation of nitrendipine loaded solid lipid nanoparticles: influence of wax and glyceride lipids on plasma pharmacokinetics. *International journal of pharmaceutics, 335*(1-2), 167–175.

Kumari, Y., Singh, S. K., Kumar, R., Kumar, B., Kaur, G., Gulati, M., & Ayinkamiye, C. (2020). Modified apple polysaccharide capped gold nanoparticles for oral delivery of insulin. *International Journal of Biological Macromolecules*.

Li, H., Zhang, M., & Ma, G. (2010). Hypolipidemic effect of the polysaccharide from Pholiota nameko. *Nutrition, 26*(5), 556–562.

Lin, W., Huang, Y.-w., Zhou, X.-D., & Ma, Y. (2006). In vitro toxicity of silica nanoparticles in human lung cancer cells. *Toxicology and applied pharmacology, 217*(3), 252–259.

Mahesh, K. V., Singh, S. K., & Gulati, M. (2014). A comparative study of top-down and bottom-up approaches for the preparation of nanosuspensions of glipizide. *Powder Technology, 256*, 436–449.

Malvindi, M. A., Brunetti, V., Vecchio, G., Galeone, A., Cingolani, R., & Pompa, P. P. (2012). SiO 2 nanoparticles biocompatibility and their potential for gene delivery and silencing. *Nanoscale, 4*(2), 486–495.
Mohsin, K., Alamri, R., Ahmad, A., Raish, M., Alanazi, F. K., & Hussain, M. D. (2016). Development of self-nanoemulsifying drug delivery systems for the enhancement of solubility and oral bioavailability of fenofibrate, a poorly water-soluble drug. *International journal of nanomedicine, 11*, 2829.
Muthyala, J., Singh, S. K., Gulati, M., Kumar, B., Rathee, H., Ghai, D., & Renuka. (2016). Systematic development and characterization of liquisolid compacts of atorvastatin-glipizide binary mixture to achieve enhanced dissolution and stability profile. *Asian Journal of Pharmaceutics, 10*(4), S1.
Ozone, F., Inoue, Y., Shiraishi, A., Hamashima, H., Masuda, K., Shiojima, K., … Sasatsu, M. (2002). Purification and characterization of 3, 3-dihydroxyazetidine from culture medium of Bacillus mesentericus and B. subtilis. *Journal of microbiological methods, 50*(1), 91–95.
Pandey, N. K., Sehal, H. R., Garg, V., Gaur, T., Kumar, B., Singh, S. K., & Rajesh, S. Y. (2017). Stable Co-crystals of Glipizide with Enhanced Dissolution Profiles: Preparation and Characterization. *Aaps PharmSciTech, 18*(7), 2454–2465.
Popoff, M. (1984). Selective medium for isolation of Clostridium butyricum from human feces. *Journal of clinical microbiology, 20*(3), 417–420.
Rajesh, S. Y., Singh, S. K., Pandey, N. K., Sharma, P., Bawa, P., Kumar, B., … Singh, S. (2018). Impact of various solid carriers and spray drying on pre/post compression properties of solid SNEDDS loaded with glimepiride: in vitro-ex vivo evaluation and cytotoxicity assessment. *Drug development and industrial pharmacy, 44*(7), 1056–1069.
Renuka, S., Kumar, Sachin, Gulati, M., & Kaur, I. (2014). Characterization of solid state forms of glipizide. *Powder Technology, 264*, 365–376.
Savjani, K. T., Gajjar, A. K., & Savjani, J. K. (2012). Drug solubility: importance and enhancement techniques. *ISRN pharmaceutics, 2012*.
Shah, V. P., Tsong, Y., Sathe, P., & Liu, J.-P. (1998). In vitro dissolution profile comparison—statistics and analysis of the similarity factor, f2. *Pharmaceutical research, 15*(6), 889–896.
Shakeel, F., Haq, N., Alanazi, F. K., & Alsarra, I. A. (2014). Polymeric solid self-nanoemulsifying drug delivery system of glibenclamide using coffee husk as a low cost biosorbent. *Powder Technology, 256*, 352–360.
Sharma, P., Singh, S. K., Pandey, N. K., Rajesh, S. Y., Bawa, P., Kumar, B., & Yadav, A. K. (2018). Impact of solid carriers and spray drying on pre/post-compression properties, dissolution rate and bioavailability of solid self-nanoemulsifying drug delivery system loaded with simvastatin. *Powder Technology, 338*, 836–846.
Simpson, P., Stanton, C., Fitzgerald, G., & Ross, R. (2005). Intrinsic tolerance of Bifidobacterium species to heat and oxygen and survival following spray drying and storage. *Journal of applied microbiology, 99*(3), 493–501.
Singh, B., Bandopadhyay, S., Kapil, R., Singh, R., & Katare, O. P. (2009). Self-emulsifying drug delivery systems (SEDDS): formulation development, characterization, and applications. *Critical Reviews™ in Therapeutic Drug Carrier Systems, 26*(5).
Singh, S., Pathak, K., & Bali, V. (2012). Product development studies on surface-adsorbed nanoemulsion of olmesartan medoxomil as a capsular dosage form. *Aaps PharmSciTech, 13*(4), 1212–1221.
Singh, S. K., Prasad Verma, P. R., & Razdan, B. (2010). Glibenclamide-loaded self-nanoemulsifying drug delivery system: development and characterization. *Drug development and industrial pharmacy, 36*(8), 933–945.
Singh, S. K., Srinivasan, K., Gowthamarajan, K., Prakash, D., Gaikwad, N. B., & Singare, D. S. (2012). Influence of formulation parameters on dissolution rate enhancement of glyburide using liquisolid technique. *Drug development and industrial pharmacy, 38*(8), 961–970.
Singh, S. K., Srinivasan, K., Gowthamarajan, K., Singare, D. S., Prakash, D., & Gaikwad, N. B. (2011). Investigation of preparation parameters of nanosuspension by top-down media milling to improve the dissolution of poorly water-soluble glyburide. *European Journal of Pharmaceutics and Biopharmaceutics, 78*(3), 441–446.
Singh, S. K., Srinivasan, K., Singare, D. S., Gowthamarajan, K., & Prakash, D. (2012). Formulation of ternary complexes of glyburide with hydroxypropyl-β-cyclodextrin and other solubilizing agents and their effect on release behavior of glyburide in aqueous and buffered media at different agitation speeds. *Drug development and industrial pharmacy, 38*(11), 1328–1336.
Singleton, V. L., & Rossi, J. A. (1965). Colorimetry of total phenolics with phosphor molybdic- phospho tungstic acid reagents. *American Journal of Enology and Viticulture, 16*, 144–158.
Süle, J., Kōrösi, T., Hucker, A., & Varga, L. (2014). Evaluation of culture media for selective enumeration of bifidobacteria and lactic acid bacteria. *Brazilian journal of Microbiology, 45*(3), 1023–1030.
Veljović, S., Veljović, M., Nikićević, N., Despotović, S., Radulović, S., Nikšić, M., … Filipović, L. (2017). Chemical composition, antiproliferative and antioxidant activity of differently processed Ganoderma lucidum ethanol extracts. *Journal of Food Science and Technology, 54*(4), 1312–1320.
Wasser, S. P. (2017). Medicinal mushrooms in human clinical studies. Part I. Anticancer, oncoimmunological, and immunomodulatory activities: a review. *International journal of medicinal mushrooms, 19*(4).
Zhang, P., Liu, Y., Feng, N., & Xu, J. (2008). Preparation and evaluation of self-microemulsifying drug delivery system of oridonin. *International journal of pharmaceutics, 355*(1-2), 269–276.
Zoeller, T., Dressman, J. B., & Klein, S. (2012). Application of a ternary HP-β-CD-complex approach to improve the dissolution performance of a poorly soluble weak acid under biorelevant conditions. *International journal of pharmaceutics, 430*(1-2), 176–183.